

**THE UNIVERSITY OF CALGARY**

**THE EFFECT OF EGF ON ENTEROCYTE NUTRIENT ABSORPTION,  
MEMBRANE FUNCTION AND SURFACE AREA**

**by**

**Jason K. Wong**

**A THESIS**

**SUBMITTED TO THE FACULTY OF GRADUATE STUDIES  
IN PARTIAL FULFILMENT OF THE REQUIREMENTS FOR THE  
DEGREE OF MASTER OF SCIENCE**

**DEPARTMENT OF GASTROINTESTINAL SCIENCES**

**CALGARY, ALBERTA**

**MARCH, 1997**

**© Jason K. Wong 1997**



National Library  
of Canada

Acquisitions and  
Bibliographic Services

395 Wellington Street  
Ottawa ON K1A 0N4  
Canada

Bibliothèque nationale  
du Canada

Acquisitions et  
services bibliographiques

395, rue Wellington  
Ottawa ON K1A 0N4  
Canada

*Your file* *Votre référence*

*Our file* *Notre référence*

**The author has granted a non-exclusive licence allowing the National Library of Canada to reproduce, loan, distribute or sell copies of his/her thesis by any means and in any form or format, making this thesis available to interested persons.**

**The author retains ownership of the copyright in his/her thesis. Neither the thesis nor substantial extracts from it may be printed or otherwise reproduced with the author's permission.**

**L'auteur a accordé une licence non exclusive permettant à la Bibliothèque nationale du Canada de reproduire, prêter, distribuer ou vendre des copies de sa thèse de quelque manière et sous quelque forme que ce soit pour mettre des exemplaires de cette thèse à la disposition des personnes intéressées.**

**L'auteur conserve la propriété du droit d'auteur qui protège sa thèse. Ni la thèse ni des extraits substantiels de celle-ci ne doivent être imprimés ou autrement reproduits sans son autorisation.**

0-612-20862-1

## **ABSTRACT**

**The effect of EGF on the regulation of jejunal nutrient transport and brush border surface area (BBSA), and the role of actin in these EGF-induced alterations was examined in rabbit jejunal tissue. In separate experiments the role of tyrosine kinase (TK) and actin in mediating the EGF effect was examined. EGF treatment resulted in a significant ( $p < 0.001$ ) increase in glucose and proline  $V_{max}$  in brush border membrane vesicles (BBMV) which was abolished by either tyrphostin (an inhibitor of TK) or cytochalasin (an inhibitor of actin polymerization). EGF had no significant effect on basolateral transport. The increase in nutrient uptake following EGF treatment was paralleled by an increase in BBSA and total surface area, which was also inhibited with cytochalasin treatment. The findings indicate a role for TK activity, and/or actin polymerization, in EGF-induced alterations in nutrient absorption and absorptive surface area.**

## **ACKNOWLEDGMENTS**

**There are many people I would like to thank for making this all happen. First, I would like to thank my supervisor, Dr. D. Grant Gall for the continual encouragement, faith, and support throughout these studies. Second, I would like to thank Dr. James Hardin for the infinite patience and guidance demonstrated in the lab. Third, I would like to thank Dr. Jon Meddings for providing me valuable insight and challenge into the work performed in these studies.**

**I would like to thank Dr. Chris Cheeseman for performing the basolateral transport studies at the University of Alberta.**

**I would also like to thank the members of the Gall lab, who always kept the lab interesting and exciting, and to the Gastrointestinal Research Group for providing a fun atmosphere to work in.**

**Honorable mention to Brian Chung, who is a great friend, and a great guy for helping me out when I was in dire straits.**

**DEDICATION**

**TO MY FAMILY, ESPECIALLY MY PARENTS, FOR THEIR LOVE AND FOR  
ALWAYS BELIEVING IN ME**

## TABLE OF CONTENTS

Approval page.....	ii
Abstract.....	iii
Acknowledgments.....	iv
Dedication.....	v
Table of contents.....	vi
List of Figures.....	ix
List of Abbreviations.....	xi
I) INTRODUCTION.....	1
II) THE ENTEROCYTE BRUSH BORDER	
A) INTRODUCTION.....	6
B) COMPONENTS OF THE BRUSH BORDER.....	6
C) THE CONTRACTILE APPARATUS OF THE BRUSH BORDER.....	10
D) BRUSH BORDER REGULATION.....	12
III) INTESTINAL TRANSPORT PROCESSES	
A) INTRODUCTION.....	14
B) TRANSCELLULAR TRANSPORT.....	14
C) THE SODIUM COUPLED GLUCOSE	

	TRANSPORTER (SGLT1).....	20
	D) PARACELLULAR TRANSPORT.....	21
IV)	EPIDERMAL GROWTH FACTOR	
	A) THE EGF FAMILY OF GROWTH FACTORS.....	22
	B) THE EGF RECEPTOR.....	23
	C) THE EFFECTS OF EGF ON INTESTINAL TRANSPORT.....	24
	D) THE EFFECT OF EGF ON INTESTINAL BRUSH BORDER SURFACE AREA AND THE ACTIN CYTOSKELETON.....	25
	E) THE ROLE OF ACTIN AND TRANSPORT PROCESSES.....	26
V)	PURPOSE OF RESEARCH.....	27
	A) AIMS OF RESEARCH.....	29
VI)	THE EFFECT OF LUMINAL EPIDERMAL GROWTH FACTOR ON ENTEROCYTE GLUCOSE AND PROLINE TRANSPORT	
	A) INTRODUCTION.....	30

	<b>B) MATERIALS AND METHODS.....</b>	<b>31</b>
	<b>C) RESULTS.....</b>	<b>37</b>
	<b>D) DISCUSSION.....</b>	<b>45</b>
<b>VII)</b>	<b>THE ROLE OF ACTIN IN EGF-INDUCED ALTERATIONS IN ENTEROCYTE MEMBRANE FUNCTION AND SURFACE AREA</b>	
	<b>A) INTRODUCTION.....</b>	<b>52</b>
	<b>B) MATERIALS AND METHODS.....</b>	<b>53</b>
	<b>C) RESULTS.....</b>	<b>58</b>
	<b>D) DISCUSSION.....</b>	<b>69</b>
<b>VIII)</b>	<b>SUMMARY.....</b>	<b>74</b>
<b>IX)</b>	<b>FUTURE DIRECTIONS OF RESEARCH.....</b>	<b>76</b>
<b>X)</b>	<b>REFERENCES.....</b>	<b>78</b>



## LIST OF FIGURES

II-1	Schematic of the intestinal brush border.....	7
VI-1	Glucose transport rates obtained from EGF-treated and control BBMVs.....	39
VI-2	Proline transport rates obtained from EGF-treated and control BBMVs.....	40
VI-3	Glucose transport rates obtained from EGF + TYR- treated and control BBMVs.....	43
VI-4	Glucose transport rates obtained from TYR-treated and control BBMVs.....	44
VII-1	Glucose transport rates obtained from EGF-treated and control BBMVs.....	59
VII-2	Kinetic parameters for glucose uptake into BBMVs obtained from EGF-treated and control tissue.....	60
VII-3	Kinetic parameters for glucose uptake into BBMVs obtained from EGF+cytochalasin D-treated and control tissue.....	62
VII-4	Kinetic parameters for glucose uptake into BBMVs obtained from cytochalasin D-treated and control tissue.....	63
VII-5	Electron micrographs of representative brush border mid-villus of control, EGF, and EGF+cytochalasin D treated tissue.....	64

<b>VII-6</b>	<b>Microvillus, height, width, density, and surface area of jejunal loops from EGF, EGF+cytochalasin D treated tissue compared to control.....</b>	<b>66</b>
<b>VII-7</b>	<b>Total absorptive surface area as % of control.....</b>	<b>67</b>

## LIST OF ABBREVIATIONS

<b>ATP</b>	<b>adenosine triphosphate</b>
<b>BB</b>	<b>brush border</b>
<b>BBMV</b>	<b>brush border membrane vesicles</b>
<b>BBSA</b>	<b>brush border surface area</b>
<b>CON</b>	<b>control</b>
<b>CYTO</b>	<b>cytochalasin</b>
<b>DAG</b>	<b>diacyl glycerol</b>
<b>DMSO</b>	<b>dimethyl sulfoxide</b>
<b>EGF</b>	<b>epidermal growth factor</b>
<b>EGFr</b>	<b>epidermal growth factor receptor</b>
<b>K<sub>m</sub></b>	<b>affinity constant</b>
<b>MLCK</b>	<b>myosin light chain kinase</b>
<b>PLC</b>	<b>phospholipase C</b>
<b>SGLT1</b>	<b>sodium coupled glucose transporter</b>
<b>TGF</b>	<b>transforming growth factor</b>
<b>TMA-DPH</b>	<b>1-[4-(trimethylamino)phenyl]-6-phenylhexatriene</b>
<b>TSA</b>	<b>total surface area</b>
<b>TYR</b>	<b>tyrphostin</b>
<b>V<sub>max</sub></b>	<b>maximal transport rate</b>

## **I. INTRODUCTION**

**The small intestine is the primary site of absorption of ingested nutrients, water, and electrolytes. To perform such a complex function the small intestine is structurally arranged into many layers. The layers from superficial to deep are the mucosa, submucosa, and circular and longitudinal smooth muscle layers. The mucosa can be further divided into an epithelial layer, lamina propria, and muscularis mucosa. The most superficial layer of the intestinal mucosa consists of a single layer of epithelial cells that provides a barrier between the external environment, the intestinal lumen, and the internal environment or body of the organism. The intestinal epithelium is comprised of a heterogeneous population of cells separated from the lamina propria by a basement membrane and connected at their lateral margins by tight junctions which allows them to act as a functional unit. The submucosa is the next layer and its primary function is to support the mucosa and separate it from the underlying muscle layers. It also houses many different cells most notably, immunologic effector cells and nerve cells. The last two layers are the circular and longitudinal muscle layers. The circular muscle layer lies between the submucosa and the outermost longitudinal muscle layer. Both layers act together to mix and propel intestinal contents for proper digestion and absorption (20). Thus, it is the various layers of the small intestine acting in concert which promotes absorption at the interface, the intestinal epithelium, of nutrients, water, and electrolytes.**

The small intestine has many structural adaptations to maximize absorptive surface area allowing for increased efficiency of its primary function. The *plica circularis* are macroscopically visible circular folds of the underlying submucosa. In humans, these folds may extend as far as 1 cm into the lumen (63). The *plica circularis* exhibit a proximal to distal gradient and are most prominent in the jejunum. Villi are microscopic folds of mucosa that overlie the *plica circularis* and increase the absorptive surface area anywhere from 7 to 14 fold. Villi display a proximal to distal gradient being most prominent in the jejunum. Depending on the species and the area of the gut the shape and height of villi vary. In humans, villi are generally leaf- and finger-shaped in the distal duodenum and proximal jejunum, ranging from 0.5 to 0.8 mm in height, whereas villi in the ileum rarely exceed 0.5 mm in height (63). Surrounding the villi are the crypts of Lieberkuhn, the site of cell proliferation. Each crypt contains 4-16 stem cells which function to produce undifferentiated cells. Undifferentiated crypt cells migrate up the wall of the crypt onto the villus and concomitantly mature. The final structural adaptation to increase surface area is exhibited on the luminal surface of intestinal epithelial cells. The apical membrane of enterocytes is comprised of many finger like projections termed microvilli. There are approximately 1000 microvilli per enterocyte resulting in an overall increase in absorptive surface area of 14 to 40 fold (63). The many different levels involved in increasing surface area ultimately allow the small intestine to efficiently perform its absorptive functions.

The plasma membrane of the enterocyte is divided into two separate,

functionally distinct, compartments. The basolateral membrane of the enterocyte is very similar in composition to other cells types and contains an enriched fraction of  $\text{Na}^+/\text{K}^+$  ATPase required to generate the  $\text{Na}^+$  electrochemical gradient used in transport processes. The apical microvillus membrane of the enterocyte is highly specialized containing a vast array of digestive enzymes and transport proteins resulting in a high protein to lipid ratio (63). In addition, the apical membrane has a high content of glycosphingolipids generating a high cholesterol to phospholipid ratio (63,70). The high cholesterol content in the apical membrane results in a decrease in membrane fluidity and an increase in membrane rigidity. An increase in membrane rigidity results in decreased membrane permeability and overall increased stability, attributes that enhance enterocyte absorption and terminal digestion (48,63,70).

As immature enterocytes migrate onto the villus functional transport and digestive proteins are expressed, such as the sodium coupled glucose transporter and sucrase, and the enterocyte begins to differentiate. The enterocyte becomes larger, nuclear material moves toward the basal pole and the cell acquires a more columnar morphology as it progresses up the crypt-villus axis. The microvilli of the brush border increase in number and height and the glycocalyx becomes more prominent (60). Enterocytes continue to migrate up the villus until they reach the villus tip. At this point, enterocytes are sloughed off the villus tip at a rate that equals migration of immature cells up the villus, allowing for a dynamic equilibrium of cell migration and renewal. In humans, under normal physiological conditions, cell

migration up the villus and consequent sloughing off the villus tip requires 5 to 6 days in the proximal small intestine, whereas it only requires 3 days in the distal small intestine (59). This may be due to the previously mentioned proximal to distal gradient for villus height in the small intestine or to the number of crypts that feed each villus (59).

The epithelial lining of the small intestine acts as a functional barrier in part due to the apical junctional complex, or terminal bar. This apical junctional complex is made up of three distinct structures: the first and most apical structure is the zona occludens, or tight junction, followed by a central zonula adherens, or intermediate junction, and lastly by a basal macula adherens, or spot desmosome (63). The tight junctions form the key barrier in this complex, and along with the enterocyte cell membranes, form a barrier to prevent passage of unwanted material into the body. Furthermore, the tight junction plays an important role in preventing the diffusion of integral membrane proteins between the apical microvillus membrane and the basolateral membrane compartments, thereby maintaining the cell polarity required for transvectorial absorption of nutrients. Tight junctions also play a major role in passive permeability by modulating paracellular flow of solutes and fluids. Tight junctions in the crypt are more permeable compared to the villus. Furthermore, tight junctions are relatively "leaky" at the level of the jejunum and become progressively tighter towards the ileum (63).

Lying directly below the tight junction is the intermediate junction. E-cadherin, a protein specific for the intermediate junction, is a  $\text{Ca}^{2+}$  dependent molecule that

causes epithelial aggregation. Thus, it is thought that a major function of the intermediate junction may involve maintaining intraepithelial relationships (63). In addition, filaments of the terminal web primarily insert into the intermediate junction. Spot desmosomes act as focal welds joining epithelial cells together, and also provide anchoring sites for stabilizing cytoskeletal cables (63).

Before nutrients are absorbed from the intestinal lumen by enterocytes they must first pass the unstirred water layer. This layer of water lies directly over the intestinal epithelium and is a region of static fluid which decreases the absorption rate of all nutrients. The absorption of lipid-soluble nutrients is influenced by the unstirred water layer to a greater degree than water soluble nutrients. The brush border rapidly absorbs lipid soluble substances, hence, a concentration gradient occurs across the unstirred water layer (50). Passive diffusion is the main mechanism for movement across the unstirred water layer resulting in the distortion of active and passive transport processes measured *in vivo* (79).



## **II. THE ENTEROCYTE BRUSH BORDER**

### **A) INTRODUCTION**

The brush border of the enterocyte is the primary interface between the blood and ingested nutrients, water, and electrolytes. It is a highly specialized structure, consisting of a myriad of finger-like apical microvilli acting to greatly increase absorptive surface area. The brush border also plays a role in the terminal digestion of nutrients. The components that comprise the brush border include the microvillus membrane, glycocalyx, underlying brush border cytoskeleton, and associated cytoskeletal proteins (48,77). Once thought to be a static structure, there is now a substantial body of evidence supporting an active role for the brush border in the response to mucosal disease and injury and the regulation of nutrient absorption (13,14,25,80).

### **B) COMPONENTS OF THE BRUSH BORDER**

A schematic diagram of the components of the enterocyte brush border is shown in Figure II-1. The microvillus membrane contains a lining of carbohydrates which protrude from the outer leaflet of the membrane, known as the glycocalyx (48,63). In addition, the outer membrane of the brush border contains a variety of specialized integral membrane proteins not found elsewhere. Many are glycosylated

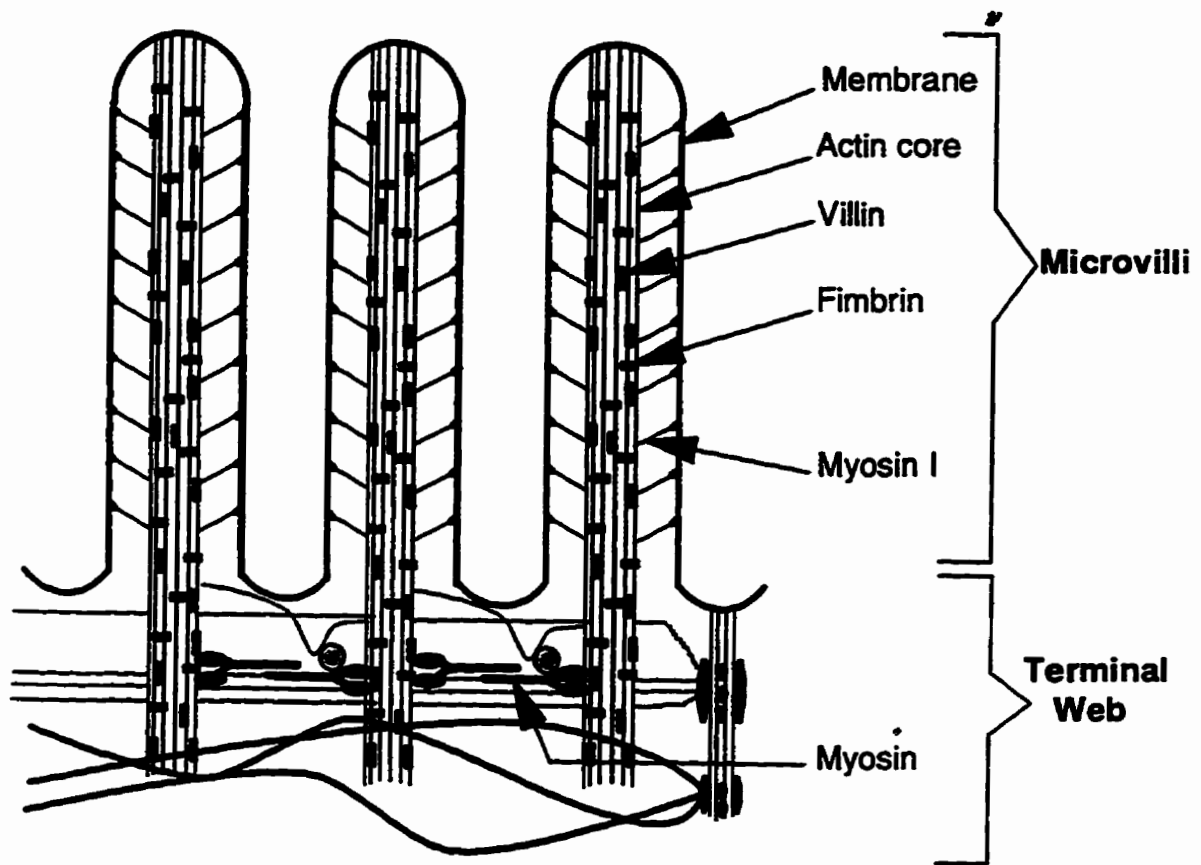


Figure II-1. The ultrastructural organization of the intestinal enterocyte brush border.

proteins, and have subsequently been identified as brush border digestive enzymes and transport proteins (48,67). Enzymes are anchored to the membrane via either a N-terminal hydrophobic sequence that spans the membrane or by a C-terminal covalent bond through a diacylglycerol (DAG) moiety (48).

The microvillus membrane is supported by the underlying terminal web cytoskeleton. The terminal web cytoskeleton is a dynamic, highly specialized, and organized structure (63,77). While comprised of a variety of different proteins the five major components of the microvillus cytoskeleton are villin, fimbrin, calmodulin, myosin-1, and actin (9,77).

Villin is a 95 kDa actin-binding protein found associated with the microvillus actin core. It is mainly produced in epithelial cells that develop a brush border and which are responsible for nutrient uptake (33). The primary function of villin is thought to be cross-linking of actin filaments into actin bundles (aggregates of actin filaments) (77). During development, assembly of the microvillus core has a strict chronological order for protein association. Villin initiates the formation of the brush border actin core bundle which is then further modified through the association of other proteins (33). In the presence of  $\text{Ca}^{2+}$ , villin has been shown to accelerate the nucleation of actin, as well as bind the barbed end of actin, thereby capping actin filaments and promoting a decrease in filament length (77). Villin also displays severing properties acting to directly cleave F-actin into actin monomers (9).

Fimbrin is a 68 kDa actin binding protein with a wide tissue distribution. Similar to villin, *in vitro* studies of fimbrin show that in the absence of  $\text{Ca}^{2+}$  it cross-

links actin filaments into uniformly polarized actin bundles that closely resemble the native microvillus core (9,77). High concentrations of  $\text{Ca}^{2+}$  inhibit the cross-linking capabilities of fimbrin by solubilizing the protein from the brush border (BB) cytoskeleton. In addition, it is thought that fimbrin plays a major role in determination of overall length of actin filaments (9).

Calmodulin and myosin-1 act in concert and together form the 110 kDa CAM complex, or BB myosin-1. BB myosin-1 makes up the lateral arms of the brush border cytoskeleton joining the plasma membrane with the actin core (9,77). Myosin-1 can also be found associated with elements of the terminal web. It is capable of traversing along actin filaments and is thought to play a role in the regulated trafficking of apical membrane proteins (1,2).

Actin is the major protein found in the brush border and the enterocyte. Actin exists in the cell in either of two states, a monomeric form known as G-actin, and a filamentous form consisting of polymerized G-actin monomers called F-actin (2). The microvillus cores are formed primarily from uniformly polarized actin filaments, with 20-30 actin filaments per microvillus core providing support for the overlying membrane (9,77). The proximal ends of the actin filaments are embedded in the terminal web and are interconnected by a network of non-core actin filaments and tropomyosin. In turn, the terminal web is laterally connected to the junctional complex.

Actin filaments are polarized structures with the barbed end, or “+” end, at the tip of the microvillus, and the pointed, or “-” end, toward the terminal web (9,77).

While actin polymerization occurs at both ends of a filament, the barbed end polymerizes much more rapidly (2,87). Polymerization of actin occurs through a three step process: initiation, nucleation, and elongation (87). Initiation is the first step in the polymerization of actin. In the presence of physiological concentrations of salt and appropriate concentrations of actin monomers, a conformational change occurs allowing the monomeric form, G-actin, to polymerize with other activated G-actins to form the filamentous form, F-actin (87). Nucleation then ensues, a slow process which is dependent on the actin monomer concentration. Polymerization of monomeric actin into a stable trimer nucleus is required before the last step in actin polymerization, elongation, occurs. Actin filaments may then anneal with one another forming a bundle of actin filaments (87).

Another protein associated with the cytoskeleton is ezrin, an 80 kDa protein that is a substrate for the EGF receptor intrinsic tyrosine kinase. When phosphorylated on tyrosine residues ezrin regulates plasma membrane structures and has been proposed to play a role in membrane insertion events (32). In parietal cells, phosphorylation of ezrin on serine/threonine residues has also been observed indicating that more than one kinase may regulate this protein (32).

### C) THE CONTRACTILE APPARATUS OF THE BRUSH BORDER

Early studies by Rodewald (1976) demonstrated an ATP-dependent contraction of the terminal web and brush border of neonatal rats (91). This was

characterized as a tightening belt around the cell at the level of the zona adherens with subsequent fanning of the microvilli into cup-shaped conformations without alterations in the length of the microvilli. In contrast, early studies by Mooseker (76) reported that, in the presence of  $\text{Ca}^{2+}$  and ATP, microvilli could be induced to retract into the terminal web causing a decrease in the length of microvilli. Subsequent studies have provided scant evidence for microvillar retraction. Brush border contraction, however, has gained considerable support (9-11,77). Contraction of the terminal web occurs on a time scale of 1-10 minutes after the addition of ATP. The mechanism of brush border contraction involves BB myosin (77). Two subsets of myosin exist in the brush border, one that tightly associates with the cytoskeleton and is involved in ZA contraction, and another set found predominantly in the inter-rootlet zone whose function is yet to be determined (77). Regulation of brush border motility includes the assembly of myosin filaments and the association of myosin with the cytoskeleton. Phosphorylation of myosin light chain by MLCK provides a regulatory mechanism for brush border contractile activity. However, light chain phosphorylation in itself is insufficient for contractile activity. The presence of hydrolyzable nucleotides is also required for the ATPase to generate the force required to contract the terminal web (11).

#### **D) BRUSH BORDER REGULATION**

The brush border is a dynamic structure continuously adapting in response to the luminal environment. Studies of malabsorptive illnesses have implicated a decrease in microvillus length and a subsequent reduction in absorptive surface area as a common mechanism in the pathology of these diseases (13,14,25). Transient shortening of microvilli has also been reported in following various treatments, including cycloheximide treatment (58), colchicine (15), and fasting animals (74). Studies in hens have reported increases in brush border surface area in the small intestine in response to a low sodium diet (97). Furthermore, in sea urchin eggs, fertilization results in a tremendous elongation of microvilli, mediated through a process involving polymerization of pre-existing actin monomers (101).

The mechanism whereby microvillus length is regulated still remains to be determined. Mooseker (1982) demonstrated that addition of excess actin monomers to isolated brush borders causes an increase in the length of microvilli actin cores (78). In developing chicken intestinal microvilli, dramatic increases in monomeric G-actin has been shown to drive microvilli elongation (101). These findings suggest that actin or actin binding proteins may play a central role in brush border regulation.

As mentioned above, villin, a protein unique to microvillar structures, possesses actin filament severing properties and actin bundling properties suggesting a regulatory role in the brush border. When human cDNA encoding villin is transfected into CV1 cells, a cell line which normally does not possess a brush

border or express villin, it causes the generation of microvilli on the cell surface and a concomitant redistribution of F-actin (33). Thus, synthesis of large amounts of villin in CV1 cells induces the formation of microvilli on those cell surfaces suggesting that villin plays a key role in the formation of microvilli.

Myosin I, a protein capable of hydrolyzing ATP to ADP when stimulated by binding to actin filaments, is also a candidate for brush border regulatory function. Myosin I has been demonstrated to possess mechanochemical motor properties allowing it to move a vesicle along an actin filament, join an actin filament to the plasma membrane, or connect two actin filaments and allow them to slide past one another (2).

Ezrin, a widely distributed actin binding protein, may also play a role in brush border regulation. Addition of EGF to A431 cells stimulates tyrosine and serine phosphorylation of ezrin. Phosphorylation of ezrin occurs concomitant with the generation of surface structures resembling microvilli within one minute of EGF treatment (9).



### **III. INTESTINAL TRANSPORT PROCESSES**

#### **A) INTRODUCTION**

As previously mentioned, the single layer of cells that comprises the intestinal epithelium, in conjunction with the tight junctions, forms a barrier separating the luminal compartment and the internal environment. Vectorial transport of solutes across the intestinal epithelium occurs via two main routes, transcellular transport and paracellular transport. Transcellular transport involves the movement of solute across the plasma membrane of an epithelial cell through the cytoplasm, and extrusion of the solute across the opposite pole of the cell. Paracellular transport refers to the movement of solute between epithelial cells without traversing the cellular plasma membrane. Transport by way of the paracellular pathway requires solutes to move across the tight junctional complex. There is a body of evidence to suggest tight junctional complexes are dynamic, opening and closing to facilitate the absorption of solutes (63).

#### **B) TRANSCELLULAR TRANSPORT**

Transcellular transport is thought to be the main pathway whereby nutrients are absorbed. Transport via the transcellular routes can occur by either an active or a passive process. Active transport provides an energy-dependent mechanism

to accumulate electrolytes or solutes against an electrochemical gradient. Active transport mechanisms involve specific membrane carrier proteins (34,114). As discussed below, active transport in intestinal epithelial cells is primarily coupled, either directly or indirectly, to the movement of sodium.

The driving force for active transport across the intestinal epithelium is the hydrolysis of ATP by the  $\text{Na}^+/\text{K}^+$ -ATPase. This enzyme is expressed in the basolateral membrane of enterocytes and transports 3  $\text{Na}^+$  ions out of the cell for every 2  $\text{K}^+$  ions transported into the cell at the cost of 1 molecule of ATP (79). As a result, there is a large inwardly-directed  $\text{Na}^+$  gradient across the enterocyte cell membrane (34,114).  $\text{K}^+$  channels on the basolateral membrane allow passive diffusion of  $\text{K}^+$  out of the enterocyte down its concentration gradient (79). The intracellular concentration of  $\text{Na}^+$  is relatively constant as increased levels of  $\text{Na}^+$  stimulate  $\text{Na}^+/\text{K}^+$ -ATPase activity resulting in a decrease in intracellular concentrations of  $\text{Na}^+$ .

Transcellular passive transport mechanisms also involve membrane carrier proteins, but in this case the carriers act to facilitate the movement of solute across the intestinal epithelium down its concentration gradient (20).

Transcellular active transport can be either absorptive or secretory. Absorptive processes move nutrients or electrolytes from the lumen into the blood, while, secretion involves the movement of solutes from the blood into the intestinal lumen (79).

In the small intestine, the major electrolytes transported are  $\text{Na}^+$  and  $\text{Cl}^-$ .  $\text{Na}^+$

ions, which drive active transport, can be absorbed by three different mechanisms:

a) electrogenic  $\text{Na}^+$  absorption, b) electroneutral  $\text{NaCl}$  absorption, and c)  $\text{Na}^+$ -coupled solute absorption.

a) Electrogenic  $\text{Na}^+$  absorption occurs throughout the small intestine and colon.  $\text{Na}^+$  crosses the brush border membrane via diffusion down its electrochemical gradient through transport proteins found in the brush border and is actively pumped out the basolateral side by the  $\text{Na}^+/\text{K}^+$  - ATPase. This flux of  $\text{Na}^+$  ions generates a serosal side positive potential difference, which is responsible for passive  $\text{Cl}^-$  absorption. The main route of passive  $\text{Cl}^-$  absorption is thought to occur by paracellular pathways, with only a small proportion of  $\text{Cl}^-$  ions using the transcellular pathway (79). Electrogenic  $\text{Na}^+$  absorption, although distributed throughout the entire gut, is not a major mechanism of  $\text{Na}^+$  absorption in the small intestine.

b) An important route of  $\text{Na}^+$  entry is electroneutral  $\text{NaCl}$  absorption, which involves the coupled movement of both ions across the brush border membrane. Entry of  $\text{Na}^+$  and  $\text{Cl}^-$  are thought to be indirectly coupled, utilizing both the  $\text{Na}^+/\text{H}^+$  exchanger and the  $\text{Cl}^-/\text{HCO}_3^-$  exchanger (79). Again,  $\text{Na}^+$  is pumped out the basolateral side by the  $\text{Na}^+/\text{K}^+$  - ATPase.  $\text{Cl}^-$  passively diffuses out the basolateral side expedited by an antiport process. This process does not occur in the jejunum where active  $\text{Cl}^-$  absorption is absent but is an important mechanism for electrolyte absorption in the ileum (20).

c) Absorption of  $\text{Na}^+$  across the brush border can be coupled to absorption of nutrients like carbohydrates, such as glucose, amino acids, and water soluble vitamins. Solute is coupled with  $\text{Na}^+$  by specific transport proteins, the driving force for absorption being the movement of  $\text{Na}^+$  down its electrochemical gradient (34,114). Efflux across the basolateral side of the cell occurs by way of facilitated diffusion. The majority of nutrients are absorbed in the jejunum, hence,  $\text{Na}^+$ -coupled transport is a prominent mechanism in this region.

Mammalian small intestine also possesses the ability to secrete electrolytes and water into the intestinal lumen. Intestinal  $\text{Cl}^-$  secretion is thought to mainly occur in the region of the crypts via brush border  $\text{Cl}^-$  channels (20), although there is some evidence to suggest that mature villus enterocytes may also possess secretory function (79).  $\text{Cl}^-$  enters the cell across the basolateral membrane by the  $\text{Na}^+/\text{K}^+/\text{2Cl}^-$  symport.  $\text{Na}^+$  is then actively pumped out of the cell by the basolateral  $\text{Na}^+/\text{K}^+$  ATPase while  $\text{K}^+$  passively diffuses out basolateral  $\text{K}^+$  channels.  $\text{Cl}^-$  moves down its concentration gradient out across the brush border membrane into the lumen resulting in  $\text{Cl}^-$  secretion. This causes a further increase in the negative potential difference in the lumen inducing a passive paracellular movement of  $\text{Na}^+$  ions and water into the lumen. In the ileum and colon,  $\text{HCO}_3^-$  secretion has also been described and involves a brush border  $\text{HCO}_3^-/\text{Cl}^-$  exchange process (20).

Intestinal absorptive and secretory processes are tightly regulated by integrated signals from the enteric nervous system, immune system, and the

endocrine system. Regulatory signals can cause acute changes, a response occurring in a time period of seconds to minutes, or an adaptive response that occurs on a much larger time scale.

The enteric nervous system, a third component of the autonomic nervous system, consists of the myenteric plexus and the submucosal plexus, an integrated network of neurons along the entire gastrointestinal tract. The enteric nervous system receives input from higher levels of the central nervous system as well as intrinsic enteric nervous system reflex pathways. Enteric neurons provide modulatory signals to the small intestinal epithelial cells affecting intestinal absorption or secretory function. Generally, cholinergic stimulation results in increased secretion or decreased absorption in the small intestine. Adrenergic activation increases intestinal absorption (20). Other neuroactive factors, such as bradykinin and vasoactive intestinal polypeptide stimulate secretion, whereas somatostatin and cholecystokinin increase absorption (20). Signals generated from neural pathways may directly affect the enterocyte by binding to a specific ligand receptor on the basolateral membrane, or it may exert its effects indirectly, acting on other components of the small intestine that modulate enterocyte function.

Cytokines released from cells of the immune system can also affect enterocyte transport function. Cells that have been reported to synthesize and release mediators that regulate intestinal secretion include mast cells, macrophages, neutrophils, and fibroblasts (45).

Signal proteins that either act directly on the enterocyte or cause an indirect

effect are another major effector of enterocyte function. These signal molecules include blood borne proteins, or hormones, released from distant sites such as adrenal and thyroid glands, paracrine stimulation as in the case of endocrine cells located in the mucosa, and luminal signals from salivary, pancreatic, and biliary, and Brunner's glands secretions (20). One such agent of interest is epidermal growth factor (EGF). Administration of luminal EGF, both *in vivo* and in intact tissue sheets *in vitro*, has been shown to increase Na<sup>+</sup> coupled glucose transport in a Ca<sup>2+</sup> dependent manner (44). Furthermore, EGF is primarily found in the gastrointestinal tract and reaches high luminal concentrations after ingesting a meal (68,86). Due to its distribution and physiological delivery a major role is proposed for EGF in the regulation of enterocyte absorptive function.

Carrier-mediated transport follows Michaelis-Menten kinetics, thus, regulation of carrier-mediated transport involve alterations in the transport protein kinetic parameters,  $V_{max}$ , defined as the maximal transport rate, and/or  $K_m$ , the affinity constant. In intact tissue, changes in  $V_{max}$  are attributable to a change in any one of the following variables: a) absorptive surface area, b) the ratio of functional transporting enterocytes to non-transporting enterocytes, c) the number of transport proteins per cell, d) the electrochemical gradient, e) the rate at which the transporter translocates substrate between the luminal side of the plasma membrane and the intracellular side of the plasma membrane, f) the lipid composition of the membrane bilayer, and g) regulatory peptides.  $K_m$  is defined as the concentration at which transport is half maximal, and represents the affinity of the carrier protein for its

substrate. A change in  $K_m$  can either indicate a conformational change in the transport protein or a change in how the transport protein is configured in the plasma membrane.

### C) THE SODIUM COUPLED GLUCOSE TRANSPORTER (SGLT1)

The sodium coupled glucose transporter (SGLT1) is an integral membrane protein located in the brush border of enterocytes. There is a gradient of SGLT1 expression along the crypt-villus axis; maximal transport function begins at the level of the mid-villus and is maintained until the villus tip, where the enterocyte sloughs off the villus into the lumen (20). While SGLT1 mRNA has been detected in crypt enterocytes, SGLT1 mRNA increases above the crypt-villus junction with a concomitant rise in SGLT1 expression. SGLT1 expression and activity increases as the enterocyte matures and moves up the villus (56). SGLT1 exists as a hetero-oligomer composed of two SGLT1 domains and two RS1 domains, though the homo-oligomer, the two SGLT1 domains alone, are capable of sodium-coupled glucose transport. Each SGLT1 domain contains 662 amino acids (73 kDa), has one glycosylation site on asparagine 248, and is thought to span the membrane eleven or twelve times (56). RS1 is a novel hydrophilic protein containing 623 amino acids (67 kDa) and contains one membrane spanning hydrophobic  $\alpha$ -helix domain. The predominant part of RS1 is localized on the extracellular side of the membrane (56). RS1 is thought to modulate SGLT1 transport function by directly

interacting on the two SGLT1 domains through an unknown mechanism. Injection of RS1-cRNA and SGLT1-cRNA into *Xenopus* oocyte cells resulted in a 40 fold increase in expressed Na<sup>+</sup>-coupled glucose transport and  $V_{max}$  over that seen when SGLT1 is expressed alone (56). Two kinetically different Na<sup>+</sup>-coupled glucose transport systems have been described: a high-affinity low capacity system and a low-affinity high capacity system (20). The above described evidence has implicated RS1 as being the modulating factor for the existence of the two systems, changing the kinetics from a high-affinity low capacity system to a low-affinity high capacity system and vice versa (56).

#### D) PARACELLULAR TRANSPORT

In the small intestine, tight junctional complexes are dynamic and relatively “leaky” as characterized by low transepithelial potential differences, and low electrical resistances (63,79). As a result, the tight junctional complex does not form a complete barrier resulting in a pathway with high passive permeability for small ions and water traveling between cells. Studies suggest paracellular transport does occur and contributes to overall absorption. However, high luminal concentrations, possibly above physiological concentrations, of nutrients are required before the paracellular pathway makes a significant contribution to intestinal nutrient absorption. Thus, the physiological role of paracellular transport in intestinal nutrient absorption remains to be determined.



#### **IV. EPIDERMAL GROWTH FACTOR**

##### **A) THE EGF FAMILY OF GROWTH FACTORS:**

Growth factors are endogenous protein ligands that both regulate cellular proliferation and act to modulate a variety of cell functions by binding to specific high affinity cell surface membrane receptors. One family of growth factors is the Epidermal Growth Factor (EGF) family of ligands. At present there are five members in the EGF family encoded by different genes: EGF, Transforming Growth Factor  $\alpha$  (TGF- $\alpha$ ), Amphiregulin, Heparin binding EGF-like growth factor (HB-EGF), and Betacellulin (19,68) . All EGF related peptides are synthesized as propeptides having three distinct domains; a cytoplasmic domain, a transmembrane domain, and an extracellular domain (19). The extracellular domain contains the mature, or active, form of the peptide that is released by proteolytic cleavage. EGF-related polypeptides have common biological effects, share similar sequence homology, and bind to the same receptor, the EGF receptor (EGFr) (68). To date no subclassification of the EGF receptor has been possible. However, there is some evidence to suggest a degree of diversity in EGF receptor binding characteristics and function (28,43,46).

## **B) THE EGF RECEPTOR:**

The EGFr possesses three distinct domains: an extracellular ligand binding domain, a transmembrane segment, and an intracellular domain containing an intrinsic tyrosine kinase (7,19,68). Despite the diverse biological effects and sites of action of EGF, initiation of EGF signal transduction is apparently similar in different cells. The binding of EGF to the receptor induces an increase in affinity of receptor-receptor association resulting in dimerization of EGFr's with subsequent activation of the intrinsic tyrosine kinase causing autophosphorylation on tyrosine residues (19). Autophosphorylation has been implicated in binding adaptor proteins through their SH2 domains, a conserved region of approximately 100 residues representing recognition motifs for specific tyrosine phosphorylated peptide sequences (7). A critical lysine residue (Lys<sub>721</sub>) of the EGFr participates in ATP binding and is essential for enzymatic activity. Studies utilizing site-directed mutagenesis have demonstrated alterations in this segment of the peptide resulted in EGF binding to the EGFr with no detectable cellular responses to EGF (19). Thus, tyrosine kinase activity following ligand binding is essential in the EGF signal transduction pathway. The activated EGF receptor can act on many intracellular substrates, potentially phosphorylating tyrosine residues on many different polypeptides including diacylglycerol (DAG) kinase, phosphoinositol (PI) kinase, phosphoinositol-4-phosphate (PIP) kinase, and phospholipase C<sub>γ</sub> (PLC). Furthermore, it has also been shown to affect GTPase activating protein (GAP),

mitogen activating protein kinase (MAP), *raf* kinase, ezrin, one of the microvillar core actin binding proteins, and many other intracellular substrates (7,19,110).

### C) THE EFFECTS OF EGF ON INTESTINAL TRANSPORT :

A number of studies have demonstrated the ability of EGF to increase absorptive function in the small intestine. In our laboratory, *in vivo* studies using single pass perfusion techniques have demonstrated significant increases in absorption of Na<sup>+</sup>, Cl<sup>-</sup>, H<sub>2</sub>O, and glucose following treatment with luminal EGF. A similar increase in glucose transport was also seen following EGF treatment in *in vitro* short-circuited tissue (82). Schwartz et al. (1988) have demonstrated an increase in galactose and glycine absorption by either a luminal or a systemic infusion of EGF (96). Recently, Horvath et al. (1994) demonstrated a significant increase in glucose transport in BBMV isolated from jejunal epithelial cells incubated with EGF (49). Other investigators have reported a significant increase in glutamine and alanine transport in jejunal brush border membrane vesicles after a subcutaneous injection of EGF into adult rats. However, in this study a decrease in glucose transport was observed following EGF treatment suggesting amino acid and sugar transport are independently regulated (94). It appears that the route of administration of EGF maybe important in determining its effects on nutrient transport.

**D) THE EFFECT OF EGF ON INTESTINAL BRUSH BORDER SURFACE AREA AND THE ACTIN CYTOSKELETON:**

The primary structural function of the brush border is to increase surface area for digestion and absorption of ions and nutrients as discussed in the previous sections. Actin is a major component of the brush border. In addition, many actin binding proteins are found in the brush border which are capable of regulating the rate of polymerization of actin (33,77). Studies have demonstrated that the EGF receptor is associated with actin filaments (109) and EGF has been shown to induce actin polymerization in cultured cells (110). Phosphorylation of proteins is a common mechanism allowing regulation of intracellular processes. Many investigators have demonstrated a role for phosphorylation of actin-binding proteins in the regulation of actin polymerization (9,11,39,40). Furthermore, van Delft et al. (1995) showed that EGF treatment induces serine phosphorylation of actin resulting in an increase in actin polymerization (110). In our laboratory, previous studies have demonstrated that acute luminal administration of EGF significantly increases small intestinal brush border surface area by increasing microvillus length (41,42). Since the actin core forms the structural backbone of the microvilli and the microvillus membrane is attached to the actin core through myosin interactions, increases in brush border surface area necessitate both an increase in the length of the actin core and insertion of additional plasma membrane to maintain cellular membrane continuity.

### E) THE ROLE OF ACTIN AND TRANSPORT PROCESSES:

Increases in both brush border surface area and intestinal transport by EGF may occur through a common mechanism. Substantial evidence exists for a role for actin in the regulation of cellular transport function (73). Tsakiridis et al. (1994) demonstrated that disruption of the actin cytoskeleton inhibited insulin induced glucose transport in muscle and fat cells (106). Watson et al. (1992) reported that removal of serum caused a decrease in  $\text{Na}^+/\text{H}^+$  exchange in Caco-2 cells. Addition of cytochalasin D inhibited the decrease in  $\text{Na}^+/\text{H}^+$  exchange suggesting that intact actin filaments play a role in the regulation of the  $\text{Na}^+/\text{H}^+$  exchanger (112). In T84 cells, cAMP-mediated stimulation of  $\text{Cl}^-$  secretion occurs concomitantly with a redistribution of F-actin. Treatment with phalloidin, a stabilizer of actin filaments, resulted in a decrease in transport activity suggesting that remodelling of actin filaments is necessary for normal  $\text{Cl}^-$  transport function (69). Furthermore, it has been reported that the actin cytoskeleton plays a role in regulation of transport proteins by binding to transport proteins directly or by interacting with transport proteins indirectly by altering components of signalling pathways, for example, phospholipases or adenylate cyclase (72,73). Thus, evidence suggests that actin plays a pivotal role in transport.

## **V. PURPOSE OF RESEARCH**

In recent years, epidermal growth factor has been shown to play a prominent role in the regulation of a variety of cellular processes. EGF binds specifically with the EGF receptor to produce a biological effect. The EGF receptor possesses intrinsic tyrosine kinase activity, and to date, all EGF responses require an intact EGF receptor. EGF concentrations in the small intestine increase in response to a meal (38), and EGF receptors have been described along the entire gastrointestinal tract (104). In addition, recent reports have demonstrated the ability of EGF to stimulate intestinal nutrient absorption (49,82,94). The increase in glucose uptake  $V_{\max}$  induced by EGF requires an intact cell and is dependent on  $\text{Ca}^{2+}$  (82). Furthermore, the EGF effect occurs rapidly, within 10 minutes suggesting that protein synthesis is not involved (82).

To further define the mechanisms behind the EGF effect on nutrient transport the effect of this cytokine on nutrient transport in brush border membrane vesicles will be examined. Brush border membrane vesicles are advantageous because the activity of integral membrane transport proteins can be studied directly. Thus, studies examining glucose and proline transport in brush border membrane vesicles will help elucidate the physiological mechanisms in intact tissue and allow the determination of whether the EGF effect is specific to one type of nutrient (i.e. glucose) or a generalized phenomenon upregulating many transport processes simultaneously.

Administration of EGF has been shown to increase brush border surface area suggesting a possible mechanism in its effect on absorptive function (41). Furthermore, other studies have shown that the binding of EGF to its receptor activates at least one tyrosine kinase (19,47,68), and that the EGF receptor itself is an actin binding protein (7,109).

Actin is a major protein in the enterocyte, forming the central core of microvilli as well as being an integral component of the rest of the cytoskeleton. A number of actin binding proteins with regulatory properties are found associated with the microvillus actin core. Villin, a  $\text{Ca}^{2+}$  dependent protein, has properties that influence the length of the actin core depending on the  $\text{Ca}^{2+}$  concentration and the amount of villin present (33). Addition of excess actin monomers has also been shown to increase microvilli length (78). EGF treatment in A431 cells has resulted in phosphorylation of actin filaments with a concomitant redistribution of actin (7,110) as well as an increase in the overall length of filamentous actin (89). These studies suggest EGF may exert its effects on the enterocyte through actin causing an increase in brush border surface area and concomitant increase in nutrient transport.

This work is presented in two sections, the first examines the effect of EGF on enterocyte brush border glucose and proline transport, and the second examines the role of actin in EGF induced alterations on enterocyte brush border membrane function and surface area.

**A) AIMS OF RESEARCH**

The specific aims of this thesis were to:

- 1) determine the effect of acute EGF exposure on brush border membrane glucose and proline transport
- 2) to examine the role of actin in EGF-induced alterations in brush border function and surface area



## **VI. THE EFFECT OF LUMINAL EPIDERMAL GROWTH FACTOR ON ENTEROCYTE GLUCOSE AND PROLINE TRANSPORT**

### **A) INTRODUCTION**

**Epidermal growth factor (EGF) is a small, acid-stable gastrointestinal peptide derived from a number of sources. EGF has been identified in Paneth cells (88), saliva, bile secretions, Brunner's glands and breast milk (68). Under physiological conditions the gastrointestinal tract is exposed to concentrations of EGF in excess of 100 ng/ml due to a combination of duodenal secretion from Brunner's glands and possibly Paneth cells as well as salivary and bile secretions (38)}.**

**The EGF receptor is a transmembrane glycoprotein composed of three major regions: an extracellular hormone-binding domain, a hydrophobic transmembrane region, and a carboxy-terminal cytoplasmic domain containing intrinsic tyrosine kinase activity (68). Despite the diverse biological effects and sites of action of EGF it appears the early steps in EGF signal transduction are similar in different cells. Binding of EGF to its receptor causes an increase in receptor-receptor affinity leading to receptor dimerization and subsequent activation of the EGF-receptor tyrosine kinase (17,99). Activation of the tyrosine kinase appears to be necessary for EGF to exert its biological effects. Experiments with cells transfected with EGF receptor mutants, lacking tyrosine kinase activity but with intact ligand binding (75), as well as studies utilizing pharmacologic tyrosine kinase inhibitors (31) have**

established that tyrosine kinase activity is necessary for the generation of most biological responses measured to date.

A growing body of evidence supports a role for EGF in the regulation of intestinal transport. Physiological concentrations of luminal EGF have been demonstrated to acutely upregulate small intestinal glucose transport both *in vivo* and *in vitro* (82). EGF has also been shown to acutely upregulate brush border surface area by a mechanism which likely involves the recruitment of additional absorptive membrane (41). Upregulation of transport function via recruitment of transport proteins from intracellular pools has been described in a number of cell types (8). It is unknown whether the EGF-induced alterations in transport are a brush border response alone or whether alterations in transport function are reflected in both apical and basal poles of the enterocyte. Acute alterations in enterocyte basolateral membrane glucose transport function have been demonstrated in response to hyperglycemia (64) as well as elevated luminal hexose loads (107). The aim of the present study was to examine the effects of acute EGF exposure at the membrane level by measuring brush border and basolateral membrane hexose and amino acid transport and to determine the role of tyrosine kinase activity in EGF-regulated intestinal transport function.

## **B) MATERIALS AND METHODS**

### **1) Animal model**

New Zealand White rabbits (800-1100g) were used. Animal care and

experimental procedures followed the guidelines of the Canadian Council of Animal Care. Animals were anaesthetized with halothane, the jejunum isolated, and two blind 9-11 cm loops, separated by a 1 cm segment, were tied off distal to the ligament of Treitz. In the first series of experiments examining brush border membrane transport function three experimental protocols were performed. In the first series of experiments EGF, at a concentration of 60 ng/ml (Sigma, St. Louis, MO.) in 1 ml saline, was added to either the proximal or distal loop and saline alone added to the control loop. In a second series of experiments EGF (60 ng/ml) and tyrphostin 51 (Sigma, St. Louis, MO.) at a final concentration of 10  $\mu$ M in 1% dimethylsulfoxide (DMSO) was added to the experimental loop and the vehicle added to the control loop. In the third series of experiments 10  $\mu$ M tyrphostin alone in 1% DMSO was added to the experimental loop and vehicle added to the control loop. A concentration of 0.8  $\mu$ M tyrphostin 51 has previously been shown to result in a 50% inhibition of EGF-dependent cell proliferation (35). To obtain enough membrane to perform the kinetic analysis, animals were twinned and concurrent experiments were run. After 1 h tissue was removed, scraped of its mucosa and mucosa was pooled from the twinned loops for preparation of brush border membrane vesicles (BBMV).

Further experiments examined the effect of the  $\text{Ca}^{++}$  channel blocker verapamil (Sigma, St. Louis, MO.) on glucose uptake in BBMV isolated from EGF and saline exposed tissue. As previously described (41), following anaesthesia a cannula was inserted via the left femoral artery into the abdominal aorta to a site

adjacent to the superior mesenteric artery. Jejunal loops were prepared as above and verapamil, 0.5 mg/kg in 1 ml saline, was infused into the animal over a period of 10 min prior to exposure of the loops to either EGF or saline for 1 h. Loops were then removed and BBMVs prepared for glucose transport as described above. Location of the cannula was confirmed post mortem.

In a separate series of experiments, enterocyte basolateral membrane transport function was examined following two experimental treatments. In the first series of experiments, EGF, at a concentration of 60 ng/ml (Sigma, St. Louis, MO.) in 1 ml saline, was added to either the proximal or distal loop and saline alone added to the control loop. In the second series of experiments jejunal loops were perfused *in vivo* as previously described (82). Briefly, either the proximal or distal loop was continuously perfused with saline containing 30 mM D-glucose (Fisher Scientific Co., Fair lawn, N.J.) and 60 ng/ml EGF and the control loop was perfused with saline containing 30 mM mannitol (BDH Inc., Toronto, ONT.). As above, in order to obtain enough membrane to perform the kinetic analysis, animals were twinned and concurrent experiments were run. After 1 h tissue was removed, and mucosa from the twinned loops scraped, pooled, and then frozen in liquid nitrogen for subsequent preparation of basolateral membrane vesicles.

## 2) Preparation of brush border membrane vesicles

Brush border membrane vesicles were prepared by a calcium chloride precipitation method as previously described (55). Brush border membrane

vesicles were stored in liquid nitrogen until day of assay. All measurements were normalized to membrane protein content as determined by the method of Lowry et al. (61). Purity and basolateral contamination of membranes was assessed by determining sucrase activity by the method of Dalquist (27), and Na<sup>+</sup>/K<sup>+</sup>-ATPase activity by the method of Kelly (54), in both the initial mucosal homogenate and microvillus membrane preparations.

### 3) Preparation of basolateral membrane vesicles

Basolateral membrane vesicles were prepared using a modification of a technique developed for isolation of rat jejunal basolateral membrane vesicles from frozen mucosal scrapings (65). The position of the vesicles in the percoll gradient was confirmed using the marker enzymes Na<sup>+</sup>/K<sup>+</sup> ATPase (83), alkaline phosphatase (83), cytochrome C oxidase (24) and cytochrome C reductase (98). The only difference from the rat vesicle preparation procedure was that we routinely found the vesicles in fractions 5,6 and 7 rather than 4,5 and 6 from the percoll gradient.

### 4) Brush border membrane vesicle transport

Brush border membrane vesicle uptake of D-glucose and L-proline was assessed using a rapid filtration technique and a 5 sec time course as previously described (53,93). All chemicals were obtained from Sigma, St. Louis, Mo., except for the D-[<sup>3</sup>H]glucose and L-[<sup>3</sup>H]proline which were obtained from NEN Research

products, Dupont, Mississauga, Ont. Vesicles were re-suspended to a final concentration of 9-12 mg protein/ml in 100 mM KCl, 300 mM mannitol, and 10 mM Tris-HEPES (pH 7.5). Studies were performed under voltage-clamped conditions with the addition of 4  $\mu$ M valinomycin to the vesicle preparations prior to transport measurements.

Glucose uptake was initiated by rapidly mixing 10  $\mu$ l of vesicles with 50  $\mu$ l buffer containing a concentration of mannitol ranging from 0 to 100 mM, 100 mM NaSCN, 10 mM Tris-HEPES, 100 mM KCl (pH 7.5), 4  $\mu$ M D-[ $^3$ H]-glucose, and variable concentrations of unlabelled D-glucose ranging from 0 to 100 mM. Proline uptake was initiated by rapidly mixing 10  $\mu$ l of the vesicle preparation with 20  $\mu$ l of buffer containing a concentration of mannitol ranging from 0 to 20 mM, 150 mM NaCl, 90 mM KCl, 10 mM Tris-HEPES, 4  $\mu$ M L-[ $^3$ H]proline, and variable concentrations of unlabelled L-proline ranging from 0 to 20 mM (pH 7.5). The reaction was stopped by addition of 4 ml ice-cold stop solution containing 100 mM NaCl, 100 mM mannitol, 10 mM Tris-HEPES, 100 mM KCl (pH 7.5). The reaction solution was then rapidly filtered through a 0.45  $\mu$ m filter (Millipore/Continental Water Systems, Bedford, MA), washed twice with 3 ml stop solution, and counted in a liquid scintillation counter. The data are expressed as picomoles of D-[ $^3$ H]glucose or L-[ $^3$ H]proline taken up per minute per milligram protein.

##### 5) Brush border membrane vesicle sodium permeability

Rates of sodium influx into brush border membrane vesicles prepared from

EGF and saline exposed tissue was determined by the method of Rood et al. (92) with some modifications as previously described (70). Experiments were performed in the absence of a pH gradient or amiloride as we wished to examine membrane sodium permeability under conditions similar to those present during the glucose and proline transport studies. Vesicle preparations were voltage clamped by the addition of 4  $\mu\text{M}$  valinomycin prior to transport measurements. 30  $\mu\text{l}$  of vesicles were then mixed with 60  $\mu\text{l}$  of buffer making a final *cis* sodium concentration of 1 mM labeled with 1  $\mu\text{Ci}$  of  $\text{Na}^{22}$  (NEN Research products, Dupont, Mississauga, Ont.). After 5 s the reaction was stopped by the addition of ice cold stop solution, filtered and counted in a gamma counter. Preliminary experiments demonstrated sodium uptake was linear for at least 10 s under these experimental conditions.

#### 6) Basolateral membrane vesicle glucose transport

All glucose uptake experiments were performed using vesicles filled with potassium thiocyanate medium and an identical uptake medium. This eliminated any possible sodium-coupled uptake if brush border membrane had contaminated the preparation. Uptake of D-glucose over a concentration range of 1 to 100 mM was linear for up to 10 seconds therefore 3 second incubations were used for kinetic analysis. All experiments were performed under zero trans conditions at room temperature using vesicles at a protein concentration of 7-9 mg/ml. D-glucose uptake was corrected for diffusion by measuring L-glucose entry in each vesicle preparation. Data are expressed as nanomoles of D- $^3\text{H}$ glucose taken up per

second per milligram protein.

#### 7) Statistical analysis

Brush border membrane kinetic analysis was performed by nonlinear regression techniques as previously described (66). Sodium permeability was analyzed by paired t-test. Basolateral membrane D-glucose uptake data was analyzed for Michaelis Menten kinetics using nonlinear regression analysis (Enzfit, Elsevier). Significance levels were set at  $p < 0.01$ .

#### C) RESULTS

All brush border membrane vesicle preparations utilized had a greater than 10-fold increase in sucrase activity compared to their respective mucosal homogenates and less than 3% basolateral contamination as determined by  $\text{Na}^+/\text{K}^+$  ATPase. As described in Materials and Methods all brush border membrane kinetic transport data are presented as competitive uptake curves with the amount of labelled substrate taken up as a function of various concentrations of unlabelled substrate. The insets in the figures display the more conventional presentation of rates of total substrate uptake as a function of total substrate concentration. As shown in Figure 1, one h exposure to 60 ng/ml luminal EGF significantly ( $p < 0.001$ ) increased the  $V_{\max}$  (40%) for glucose uptake in brush border membrane vesicles (EGF  $16.1 \pm 1.0$  vs CON  $11.5 \pm 0.9$  nmol/min/mg protein;  $n=5$ ). Further



experiments were performed to determine if the observed effect of EGF on brush border glucose transport was specific for glucose absorption or reflected a more generalized upregulation of brush border transport function. The effect of EGF on brush border membrane vesicle proline transport is shown in Figure 2. Proline transport was enhanced to a similar degree (46%) to that seen for glucose in EGF treated tissue (EGF  $3.8 \pm 0.5$  vs CON  $2.6 \pm 0.3$  nmol/min/mg protein;  $p < 0.0001$ ,  $n=5$ ). The  $K_m$  for either glucose (EGF  $123 \pm 11$  vs CON  $134 \pm 15$   $\mu\text{M}$ ) or proline (EGF  $276 \pm 46$  vs CON  $293 \pm 40$   $\mu\text{M}$ ) uptake did not differ in brush border membrane vesicles from EGF-treated and control tissue.

All basolateral membrane vesicles showed at least a 17-fold enrichment in the specific activity of  $\text{Na}^+/\text{K}^+$  ATPase, with little contamination by brush border or microsomal fractions. Initial experiments examined the effect of 1 h EGF exposure on basolateral membrane glucose kinetics. No difference in either  $V_{\text{max}}$  (EGF  $1.8 \pm 0.3$  vs CON  $1.6 \pm 0.1$  nmol/sec/ mg protein) or  $K_m$  (EGF  $42 \pm 15$ ;  $n=4$  vs CON  $38 \pm 5$  mM;  $n=5$ ) was seen following exposure of jejunal tissue to luminal EGF. In order to determine whether alterations in basolateral glucose transport may be secondary to increased glucose entry across the apical pole of the enterocyte a second series of experiments was performed in which 30 mM glucose and EGF was continuously perfused through the lumen of one loop and subsequent membrane preparations compared to a control loop perfused with mannitol. The  $V_{\text{max}}$  and  $K_m$  for glucose transport did not differ between basolateral membrane preparations

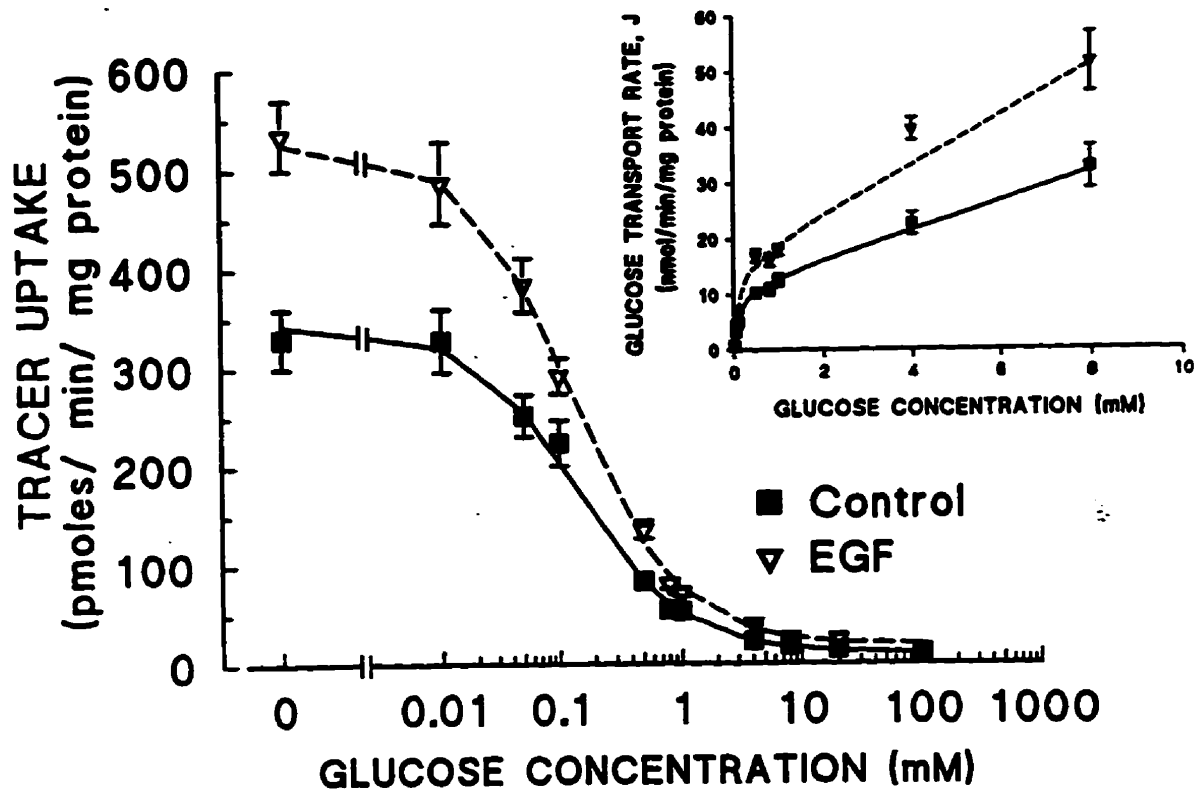


Figure VI-1. Glucose transport rates in brush border membrane vesicles obtained from EGF-treated and control tissue. Each data point represents mean  $\pm$  SE obtained in 5 membrane preparations. In each preparation measurements were performed in at least triplicate for each glucose concentration. Data shown represent the uptake of glucose in the presence of a 100 mM inwardly directed sodium gradient. Rates of D- $^3$ H]glucose uptake were plotted against the concentration of unlabelled substrate present. *Inset*: Conventional presentation of rates of total glucose uptake as a function of total glucose concentration.

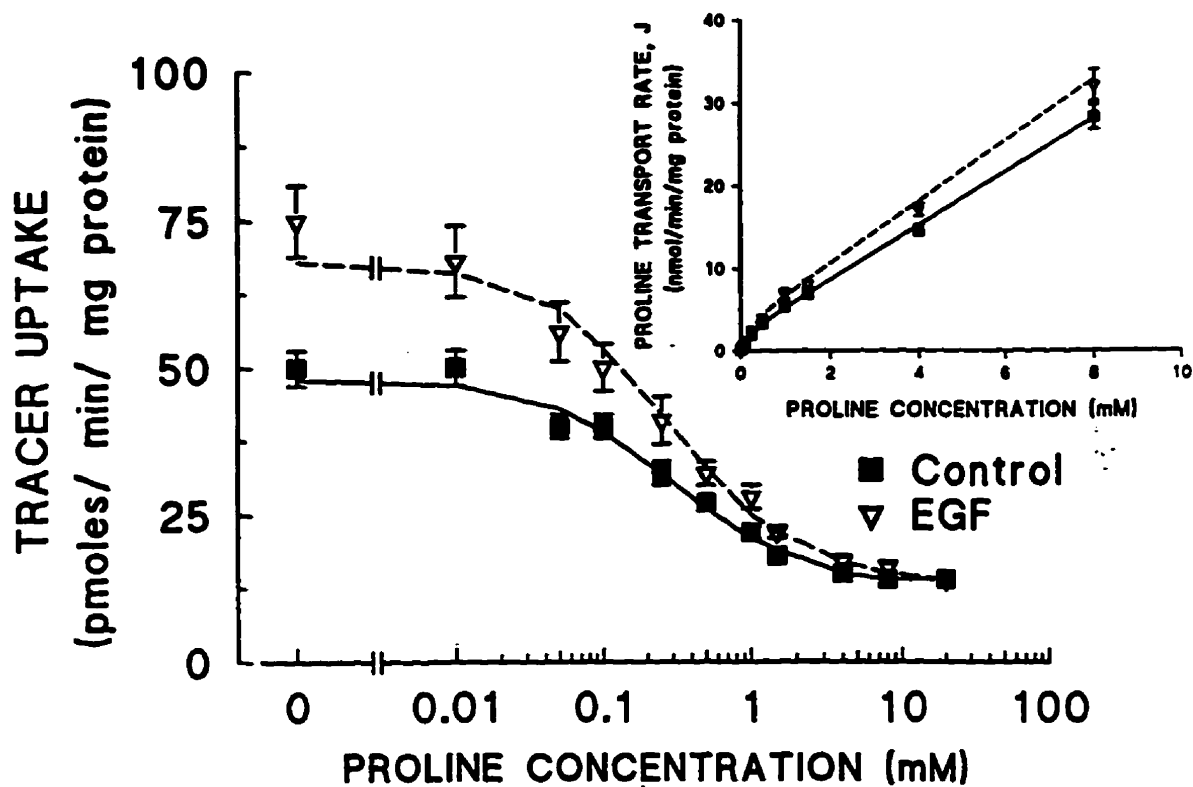


Figure VI-2. Proline transport rates in brush border membrane vesicles obtained from EGF-treated and control tissue. Each data point represents mean  $\pm$  SE obtained in 5 membrane preparations. In each preparation measurements were performed in triplicate for each proline concentration. Data shown represent the uptake of proline in the presence of a 100 mM inwardly directed sodium gradient. Rates of D- $^3$ H]proline uptake were plotted against the concentration of unlabelled substrate present. *Inset*: Conventional presentation of rates of total proline uptake as a function of total proline concentration.

from EGF and glucose treated loops compared to control membrane preparations ( $V_{\max}$  EGF  $1.3 \pm 0.1$  vs CON  $1.2 \pm 0.2$  nmol/sec/mg protein;  $K_m$  EGF  $41 \pm 7$  vs CON  $38 \pm 11$  mM;  $n=6$ ).

The role of tyrosine kinase activity in the EGF-induced upregulation of transport function was examined using the tyrosine kinase inhibitor tyrphostin 51 (TYR). As shown in Figure 3 simultaneous administration of EGF and  $10 \mu\text{M}$  tyrphostin completely abolished the EGF induced increase in glucose transport and resulted in a significant ( $p<0.0001$ ) reduction in  $V_{\max}$  compared to controls (EGF + TYR  $5.9 \pm 0.3$  vs CON  $10.7 \pm 0.6$  nmol/min/mg protein;  $n=4$ ). Subsequently, a further series of experiments investigated the role of tyrosine kinase activity in the maintenance of basal brush border membrane transport function (Figure 4). Intraluminal administration of  $10 \mu\text{M}$  tyrphostin alone resulted in a significant ( $p<0.0001$ ) reduction in the  $V_{\max}$  for glucose uptake when compared to controls (TYR  $8.0 \pm 0.8$  vs CON  $10.7 \pm 1.0$ ;  $n=4$ ). The  $K_m$  for glucose uptake in brush border membrane vesicles obtained from control loops did not differ significantly from values obtained after exposure of loops to either EGF and tyrphostin (EGF + TYR  $129 \pm 16$  vs CON  $109 \pm 7 \mu\text{M}$ ) or tyrphostin alone (TYR  $168 \pm 23$  vs CON  $161 \pm 27 \mu\text{M}$ ).

To define the role of extracellular calcium, we examined the effect of  $\text{Ca}^{++}$  channel blockade on the EGF-induced upregulation of brush border membrane transport function. Intraarterial infusion of verapamil for 10 min prior to EGF exposure abolished the EGF-induced increase in BBMV glucose uptake (EGF  $13.2$

$\pm 0.3$  vs CON  $12.4 \pm 0.5$  nmol/min/mg protein; n=4).  $K_m$  did not differ between EGF and control vesicle preparations obtained from animals infused with verapamil (EGF  $100 \pm 4$  vs CON  $124 \pm 11$   $\mu$ M).

Sodium uptake into vesicles was measured to determine if EGF treatment non-specifically altered brush border membrane vesicle sodium permeability. Sodium permeability did not differ between vesicle preparations from EGF and saline exposed tissue (EGF  $1.09 \pm 0.11$  vs CON  $1.11 \pm 0.07$  nmol/min/mg protein; n=3).

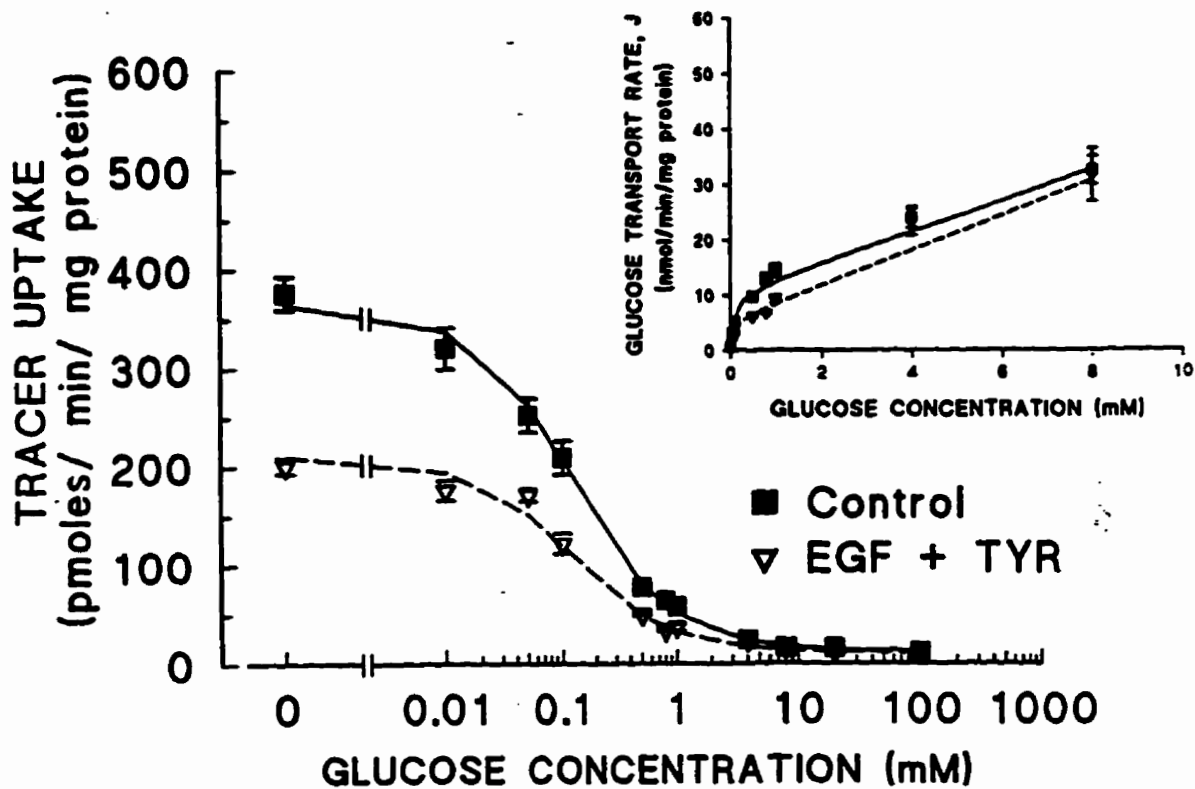


Figure VI-3. Glucose transport rates in brush border membrane vesicles obtained from EGF plus tyrphostin-treated vs control tissue. Each data point represents mean  $\pm$  SE obtained in 4 membrane preparations. In each preparation measurements were performed in at least triplicate for each glucose concentration. Data shown represent the uptake of glucose in the presence of a 100 mM inwardly directed sodium gradient. Rates of D- $^3$ H]glucose uptake were plotted against the concentration of unlabelled substrate present. *Inset*: Conventional presentation of rates of total glucose uptake as a function of total glucose concentration.

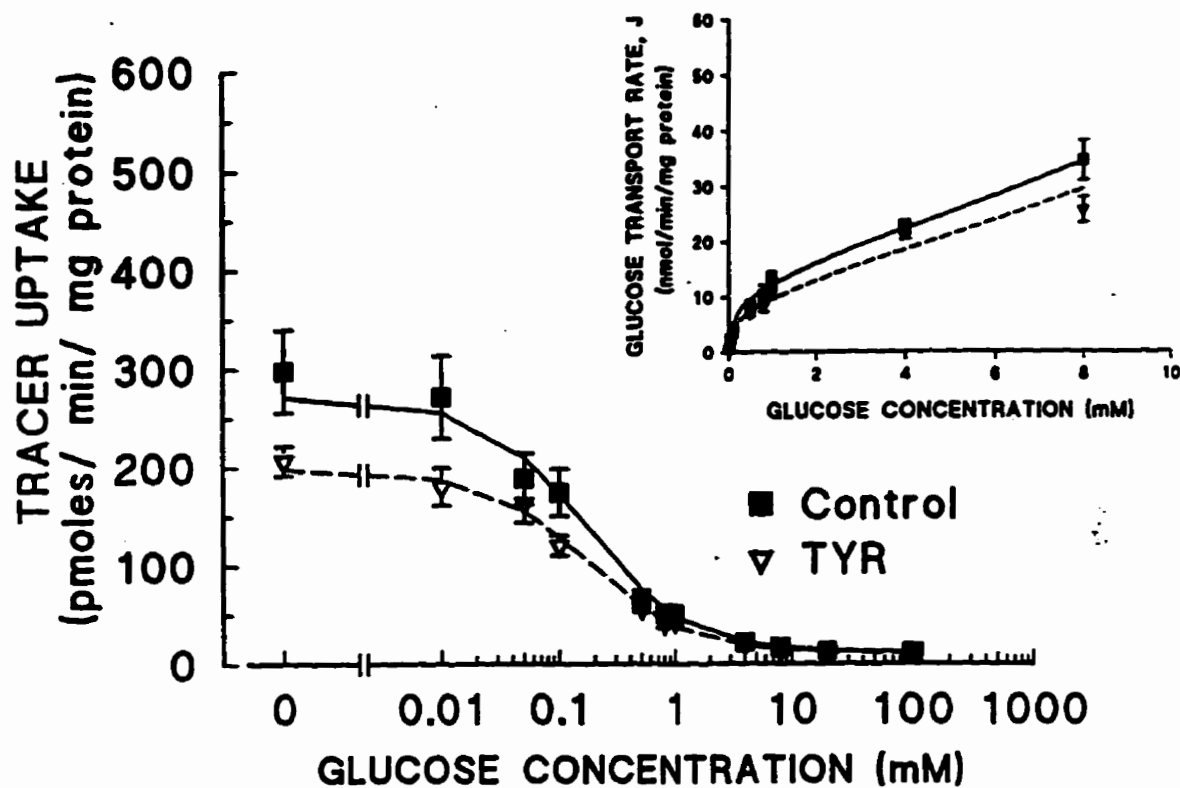


Figure VI-4. Glucose transport rates in brush border membrane vesicles obtained from tyrphostin-treated vs control tissue. Each data point represents mean  $\pm$  SE obtained in 4 membrane preparations. In each preparation measurements were performed in at least triplicate for each glucose concentration. Data shown represent the uptake of glucose in the presence of a 100 mM inwardly directed sodium gradient. Rates of D- $^3$ H]glucose uptake were plotted against the concentration of unlabelled substrate present. *Inset*: Conventional presentation of rates of total glucose uptake as a function of total glucose concentration.

#### **D) DISCUSSION**

The results suggest that epidermal growth factor can acutely upregulate the  $V_{\max}$  for brush border nutrient uptake. This EGF-induced increase in transport function is mediated by tyrosine kinase activity and dependent on extracellular calcium and, furthermore, basal tyrosine kinase activity appears to be involved in the maintenance of brush border membrane transport function.

EGF secreted from Brunner's glands and potentially Paneth cells in combination with salivary and bile secretions can expose the gastrointestinal tract to concentrations of EGF in excess of 100 ng/ml (38). In humans, salivary EGF levels show an apparent rhythm related to meals (51). EGF is relatively acid-stable and under intermediate acidic conditions passes largely intact through the stomach (85). Furthermore, EGF is resistant to digestion by pancreatic enzymes in the presence of food proteins (86). Thus, EGF's distribution and physiological delivery to the gastrointestinal tract may provide an ideal mechanism whereby nutrient absorptive function could be acutely regulated.

In a transporting epithelium, changes in  $V_{\max}$  are mainly due to a change in:

- a) the turnover rate of the transporter;
- b) the number of transport proteins per cell;
- c) the ratio of cells that have transporting capabilities vs. cells without transporting capabilities
- d) the electrochemical gradient;
- e) the physical properties of the lipid bilayer;
- f) the absorptive surface area and
- g) alteration of regulatory peptide function.



Recently, a novel protein, RS1, has been shown to regulate glucose transport. SGLT1 can exist as a hetero-oligomer, consisting of two SGLT1 domains and two RS1 domains, or a homo-oligomer, composed of two SGLT1 domains alone. When RS1 domains bind with SGLT1 domains, glucose transport is greatly enhanced (56). Thus, it is possible that the EGF-induced increase in glucose transport occurs through a mechanism involving RS1 translocation with subsequent binding to SGLT1 domains. However, the EGF-induced increase in glucose transport was not an isolated phenomenon but a more generalized mechanism for nutrient transport. Measurement of amino acid (proline) transport via the proline transporter after EGF treatment also displayed an increase in transport. Interestingly, the increase in proline transport was of a similar magnitude to that observed with glucose transport. To our knowledge, the proline transporter does not have a regulatory protein similar to that of RS1, thus, it seems unlikely that the EGF-induced mechanism involves regulatory proteins such as RS1.

In the present study EGF acutely upregulated the  $V_{max}$  for both glucose and proline. In isolated brush border membrane vesicles alterations in  $V_{max}$  may be attributed to changes in either the number of transport proteins, or the rate at which the transporter translocates substrate across the membrane. In previous studies we found no difference in brush border membrane composition or physical characteristics following EGF treatment (41). Further, in the present experiments  $K_m$  was not altered by EGF or tyrosine kinase inhibition indicating no change in transporter affinity. Additionally, sodium permeability was examined in brush border

membrane vesicles prepared from EGF-treated and control tissue and was found not to differ under similar conditions to those existing during glucose and proline transport measurements suggesting that the observed EGF-induced increase in the  $V_{\max}$  for nutrient uptake was not due to non-specific alterations in vesicle sodium permeability. Thus, it seems likely that the increase in  $V_{\max}$  following EGF treatment is due to recruitment of additional transport proteins into the microvillus membrane.

EGF has been demonstrated to acutely upregulate brush border surface area by a process that likely involves recruitment of additional preformed absorptive membrane from an intracellular pool (41). The findings in the current study suggest this preformed pool of membrane contains functional transport proteins, and that these occur in a higher concentration per membrane protein than in the brush border membrane prior to stimulation. Furthermore, due to the virtually identical levels of enhancement observed for both glucose and proline uptake following EGF treatment, this preformed pool likely contains a variety of transport proteins leading to a generalized increase in transport function following recruitment to the brush border. Such a translocation of transport proteins following stimulation by a biochemical ligand has previously been reported in a variety of cell types. In adipocytes, both insulin and EGF have been shown to stimulate translocation of  $\text{Na}^+$ -independent glucose transporters from an intracellular pool into the plasma membrane (100). Likewise, acute alterations in cellular solute transport following recruitment of preexisting transport proteins into the plasma membrane has been demonstrated in a number of tissues including the renal collecting tubule

(antidiuretic hormone responsive water channel), gastric parietal cells ( $H^+/K^+$  ATPase), and in T84 colonocytes (CFTR - secretory  $Cl^-$  channel) (8). There is conflicting evidence to support the existence of such a pool of recruitable membrane and transport proteins in enterocytes. Takata et al. (1992) demonstrated in rat jejunal enterocytes that SGLT1 transporters were only located on the apical membrane and in the Golgi apparatus (103). Recently, immunohistochemical staining for SGLT1 in human ileal tissue has demonstrated the presence of SGLT1 transporters on the apical membrane, Golgi apparatus, and in cytoplasmic secretory vesicles (113). Thus, intracellular translocation of SGLT1 transporters to the apical membrane from cytoplasmic secretory vesicles is a possible mechanism to increase glucose transport in the jejunum.

The role of EGF in the regulation of intestinal transport function is supported by a number of studies. *In vitro* glucose absorption in mice jejunal rings is upregulated following 3 days of subcutaneous EGF administration (5). Studies by Salloum et al. (94) reported an increase in the  $V_{max}$  for both glutamine and alanine uptake in rat jejunal brush border membrane vesicles following EGF treatment. In contrast, however, glucose transport was found to be simultaneously decreased in EGF-treated rats. Recently, EGF has been reported to acutely upregulate the  $V_{max}$  for brush border glucose uptake in isolated rat jejunal enterocytes (49).

In contrast to the transport alterations observed in the brush border membrane of jejunal enterocytes treated with EGF, no difference was seen in basolateral membrane glucose absorption following EGF treatment indicating that

there is no direct effect of EGF on the basolateral membrane. In order to rule out the possibility that alterations in the basolateral membrane might be secondary to increased glucose uptake across the brush border membrane we performed a second series of experiments in which EGF and 30 mM glucose was perfused through one loop and compared to a mannitol perfused loop. No difference in basolateral membrane glucose transport was seen from tissue exposed to EGF and glucose compared to mannitol-treated control tissue. Under certain conditions there is little doubt that the basolateral membrane is capable of acutely regulating glucose transport function. Increases in basolateral membrane glucose transport  $V_{max}$  have been reported after 30 min of hyperglycemia (21). Four hours of luminal hexose infusion has also been shown to result in elevations in the  $V_{max}$  for basolateral membrane glucose transport (107). Our inability to detect changes in basolateral transport function following luminal glucose perfusion may be due to the short period of glucose perfusion relative to the above mentioned studies. The lack of effect of EGF on basolateral glucose transport indicates; a) that alterations in transport function in the brush border vs the basolateral membrane compartment are not necessarily linked, and b) basolateral membrane transport function may be more sensitive to alterations in blood glucose concentrations than luminal hexose loads. The findings suggest that basolateral membrane glucose efflux is not a rate limiting step during acute EGF-induced elevations in glucose transport across the intestinal epithelium.

The experiments with the tyrosine kinase inhibitor tyrphostin 51 indicate that

EGF-induced alterations in intestinal transport are mediated by tyrosine kinase activity, and, furthermore, that basal tyrosine kinase activity is involved in the maintenance of brush border membrane transport function. The role of tyrosine kinase in transducing the EGF stimulus is not surprising given the structure of the EGF receptor and the demonstrated importance of tyrosine kinase in most of the biological effects of EGF (31,68,75). However, the possibility that tyrphostin may be acting on a tyrosine kinase distinct from the intrinsic EGF receptor linked enzyme cannot be discounted. Tyrosine phosphorylation of mitogen-activated protein kinase has been reported in cells expressing tyrosine kinase negative EGF receptor mutants following EGF stimulation (16). Luminal EGF induces the rapid tyrosine phosphorylation of both the EGF receptor and *c-neu*, a homologous tyrosine kinase in 8 day old rat pups (105). In rabbit ileum, EGF has been reported to stimulate NaCl absorption, an effect which apparently involves a brush border tyrosine kinase (30). Furthermore, ileal tyrosine kinase activity was shown to have a role in the maintenance of basal NaCl absorption and brush border Na<sup>+</sup>/H<sup>+</sup> exchange. In contrast to the current study the EGF response described in the rabbit ileum was produced only by serosal application of EGF (30). The reason for this discrepancy is unknown though this may reflect regional differences in epithelial responsiveness to EGF along the small intestine. In this regard it is noteworthy that EGF was not found to stimulate glucose uptake in the ileum though this effect has been clearly demonstrated in the jejunum (5,49,82).

Tyrosine kinase activity has also been shown to be involved in basolateral

calcium influx in colonocytes (6). In the current study verapamil, a  $\text{Ca}^{++}$  channel blocker, abolished the EGF-induced increase in  $V_{\text{max}}$  for glucose uptake. In previous studies verapamil was also found to prevent EGF-induced increases in apical absorptive surface area (41) and glucose transport in intact jejunal tissue in vitro (82). The possibility exists therefore that the tyrosine kinase activity inhibited by tyrphostin 51 may be mediating basolateral calcium entry and subsequent elevations in intracellular calcium may provide the trigger for transporter recruitment.

In summary, the findings indicate a role for EGF in the acute regulation of jejunal brush border membrane nutrient uptake. Furthermore, tyrosine kinase activity appears to have a role both in mediating EGF-induced alterations in transport function and in the maintenance of basal brush border membrane function.

**Acknowledgement:** I would like to thank Dr. Chris Cheeseman for performing the basolateral transport experiments in this chapter.

## **VII. THE ROLE OF ACTIN IN EGF-INDUCED ALTERATIONS IN ENTEROCYTE MEMBRANE FUNCTION AND SURFACE AREA**

### **A) INTRODUCTION**

Epidermal Growth Factor (EGF) is a 53 amino acid peptide derived from many sources in the gastrointestinal tract including saliva, amniotic fluid, urine, bile, Paneth cells (88), and Brunner's glands of the duodenum (68). EGF is a potent mitogen and has been shown to promote DNA synthesis (18,68) and transcription of RNA leading to protein synthesis (18). EGF has also been shown to regulate small intestinal transport function. EGF has been shown to increase intestinal nutrient and ion absorption both *in vivo* and *in vitro* (82) and this effect is associated with increases in brush border surface area and total absorptive surface area (41). In addition, our laboratory as well as others (44,49) have demonstrated an increase in  $V_{max}$  for glucose transport in jejunal brush border membranes following EGF treatment.

In order for EGF to exert its biological effects it must first bind to a specific transmembrane receptor. This receptor has three main regions: an extracellular ligand binding domain, a transmembrane segment, and an intracellular domain possessing intrinsic tyrosine kinase activity (3,68). The binding of EGF to its receptor induces dimerization of bound receptors resulting in activation of the EGF receptor complexes by autophosphorylation on tyrosine residues (99,108). The

activated EGF receptor complex has been shown to be associated with the actin cytoskeleton (29,89,109), as well as to act on many intracellular substrates, including four enzymes linked to the cytoskeleton: diacylglycerol (DAG) kinase, phosphoinositol (PI) kinase, phosphoinositol-4-phosphate (PIP) kinase, and phospholipase C<sub>γ</sub> (PLC) (84).

Activation of the EGF receptor has been reported to lead to increased F-actin content in cultured cells (89), and stimulation of cells with EGF has been shown to induce serine phosphorylation on actin filaments (110). The brush border of intestinal epithelial cells, an evolutionary adaptation designed to increase surface area for digestion and absorption of ions and nutrients, appears to be a primary site of action of EGF in the small intestine. A major component of the brush border is actin, which comprises the core of each microvillus. Actin is also known to be involved in the regulated cycling and insertion of membrane proteins including transport proteins (32,73,106). Thus, we hypothesized that EGF increases nutrient and ion absorption by increasing brush border surface area through a mechanism involving the polymerization of actin. The aim of the present study was to assess the role of actin in EGF-induced alterations in membrane function and surface area.

## **B) MATERIALS AND METHODS**

### **1) Animal Model**

New Zealand White rabbits (800-1000 g) were used. Experimental



procedures followed standards set by the Canadian Council of Animal Care. Animals were anaesthetized with halothane, a laparotomy performed, jejunum isolated, and two blind 10-15 cm loops, separated by a 1 cm segment, were tied off 5 cm distal to the ligament of Treitz. Three separate experimental conditions were examined; either EGF (60 ng/ml) (Sigma, St. Louis, MO) in 1.8-2.0 ml of Krebs buffer [(in mM) 140 Na<sup>+</sup>, 127.5 Cl<sup>-</sup>, 25 HCO<sub>3</sub><sup>-</sup>, 10 K<sup>+</sup>, 1.25 Ca<sup>2+</sup>, 1.1 Mg<sup>2+</sup>, 2 H<sub>2</sub>PO<sub>4</sub>, pH 7.4], EGF (60 ng/ml) and cytochalasin D (2 μM) (Sigma, St. Louis, MO) in 1.8-2.0 ml of Krebs buffer, or cytochalasin D (2 μM) alone in 1.8-2.0 ml of Krebs buffer. Experimental solutions were added alternately to either the proximal or distal loop and vehicle alone, 0.1% dimethyl sulfoxide (DMSO) in 1.8-2.0 ml of Krebs buffer, added to the remaining loop. Cytochalasins have previously been shown to effectively inhibit actin polymerization (12,23,81). In separate experiments, loops were harvested after 1 h for determination of brush border membrane vesicle glucose transport or brush border surface area, or in loops treated with EGF or EGF plus cytochalasin for measurement of total absorptive surface area.

## 2) Brush border membrane vesicle glucose transport

To obtain sufficient membrane to perform the kinetic analysis, animals were twinned, and concurrent experimental treatments were run. After a 1 h incubation, loops were removed, scraped of mucosa, and brush border membrane vesicles prepared by a calcium chloride precipitation method as previously described (52). Brush border membrane vesicles were stored in liquid nitrogen until day of assay.

All measurements were normalized to membrane protein, as determined by the method of Lowry et al. (61). Purity of brush border membranes was evaluated by measuring sucrase activity in both the initial mucosal homogenate and the microvillus membrane preparation. Sucrase activity was determined by the method of Dalquist (27). Basolateral contamination was assessed by comparing  $\text{Na}^+/\text{K}^+$  ATPase activity in the initial homogenate and the microvillus preparation by the method of Kelly (54).

Brush border membrane vesicle uptake of D-glucose was measured using a rapid filtration technique and a 5 sec time course as previously described (53). All chemicals were obtained from Sigma, St. Louis, MO., except for the D- $^3\text{H}$  glucose which was obtained from NEN Research products, Dupont, Mississauga, Ont. Vesicles were resuspended to a final concentration of 8-15 mg protein/ml in 100 mM KCl, 300 mM mannitol, and 10 mM Tris-HEPES (pH 7.5). Valinomycin (4  $\mu\text{M}$ ) was added immediately prior to transport measurements to voltage-clamp the vesicle preparations.

Glucose transport was measured by mixing 10  $\mu\text{l}$  of membrane vesicles with 50  $\mu\text{l}$  reaction buffer containing a concentration of mannitol ranging from 0 to 100 mM, 100 mM NaSCN, 10 mM Tris-HEPES, 100 mM KCl (pH 7.5), 4  $\mu\text{M}$  D- $^3\text{H}$ -glucose, and variable concentrations of unlabeled D-glucose ranging from 0 to 100 mM. Glucose transport was stopped by addition of 5 ml ice-cold stop solution (100 mM NaCl, 100 mM mannitol, 10 mM Tris-Hepes, 100 mM KCl, pH 7.5). The solution was then rapidly filtered through a 0.45  $\mu\text{m}$  filter (Millipore/Continental Water

Systems, Bedford, MA), and washed with 5 ml of stop solution. Filters were placed in 10 ml scintillation fluid and counted in a liquid scintillation counter. Brush border membrane kinetic analysis was performed by nonlinear regression techniques as previously described (66). Data are expressed as nanomoles of D- $^3\text{H}$ ] glucose taken up per minute per milligram protein.

### 3) Surface Area Determination

Transmission electron microscopy: Jejunal brush border surface area was determined from three animals for each treatment group. After a 1 h incubation, EGF, EGF+cytochalasin D, cytochalasin D alone or control loops were removed and fixed in 5% glutaraldehyde in phosphate buffer [(in M) 0.2  $\text{NaH}_2\text{PO}_4$ , 0.2  $\text{Na}_2\text{HPO}_4$ , pH 7.3], osmolality 300 mosmol/kg  $\text{H}_2\text{O}$  at 20<sup>o</sup> C. Tissue was postfixed in 1%  $\text{OsO}_4$  for 2 h, dehydrated in graded alcohols, cleared with propylene oxide, and infiltrated with and embedded in Spurr's low viscosity medium (J. B. EM services, Dorval, Canada). Ultra-thin sections were obtained and double stained with uranyl acetate in 50% ethanol and 0.4% lead citrate (111). Micrographs were obtained from the midvillus region of the sections as determined by a low-magnification observation of complete villi. Duplicate measurements from each micrograph were obtained and jejunal midvillus brush border area was calculated as previously described (13). To avoid observer bias, the study was performed under blinded conditions.

TMA-DPH equilibration: As previously described (41), the impermeant fluorophore 1-[4-(trimethylamino)phenyl]-6-phenylhexatriene (TMA-DPH) was used

to measure the apical membrane surface area of in vivo jejunal loops exposed to either EGF, EGF+cytochalasin D, or vehicle control. Briefly, unsealed erythrocyte ghosts were prepared as described by Steck (57), labeled with 10  $\mu$ M TMA-DPH in DMSO, and subsequently washed to remove unbound probe. We have previously shown TMA-DPH equilibrates between ghosts and enterocyte apical membranes by 10 min in jejunal loops (41). Surgeries were performed as above and after a 50 min incubation of experimental solutions in the jejunal loops, approximately  $130 \times 10^6$  ghosts in 1 ml Krebs buffer were injected into the loops and allowed to equilibrate for 10 min. After 10 min, ghosts were removed and the loops were excised for determination of length. The size and number of the unsealed erythrocyte ghosts was then determined by coulter counter (model ZM, Coulter Electronics, Luton, Bedford, UK) and total fluorescence was assessed by an SLM AMINCO SPF-500C spectrophotometer (Urbana, IL). Total absorptive surface area was then calculated as previously described (41).

#### 4) Statistical Analysis

Data are expressed as mean  $\pm$  SE and statistical analyses were performed by Student's t-test or analysis of variance with repeated measurements. Statistical comparison of kinetic curves was performed as previously described (71). Significance levels were set at 0.01 for kinetic analysis and at 0.05 for comparison of brush border and total surface area parameters.

## C) RESULTS

### 1) Glucose Kinetics

Jejunal brush border membrane vesicles prepared from EGF, EGF+Cytochalasin D, and Cytochalasin D treated loops were compared to control vesicle preparations. All brush border membrane vesicle preparations used in this study demonstrated at least a 10-fold increase in sucrase activity compared to their respective mucosal homogenates and less than a 3% basolateral contamination as determined by  $\text{Na}^+/\text{K}^+$  ATPase. Figure 1 displays kinetic transport data for the EGF vs. control treatment group as competitive uptake curves where the amount of labeled tritiated glucose transported into the vesicle is a function of various concentrations of unlabeled glucose. For ease of interpretation kinetic parameters for the uptake of glucose into brush border vesicles have been calculated and are presented in Figures 2-4. Luminal exposure of tissue to 60 ng/ml EGF for 1 h resulted in a significant ( $p < 0.001$ ) increase in the  $V_{\max}$  (33%) for glucose transport in brush border membrane vesicles (EGF  $14.6 \pm 0.6$  vs CON  $11.0 \pm 0.9$  nmol/min/mg protein;  $n=7$ ) (Figure 2). To determine the role of actin in the EGF-induced increase in glucose transport, an inhibitor of actin polymerization, cytochalasin D (2  $\mu\text{M}$ ), was concurrently administered with EGF. As shown in Figure 3, glucose transport kinetics in vesicles from EGF+Cytochalasin D treated tissue did not significantly differ from vesicles obtained from control tissue (EGF+Cytochalasin

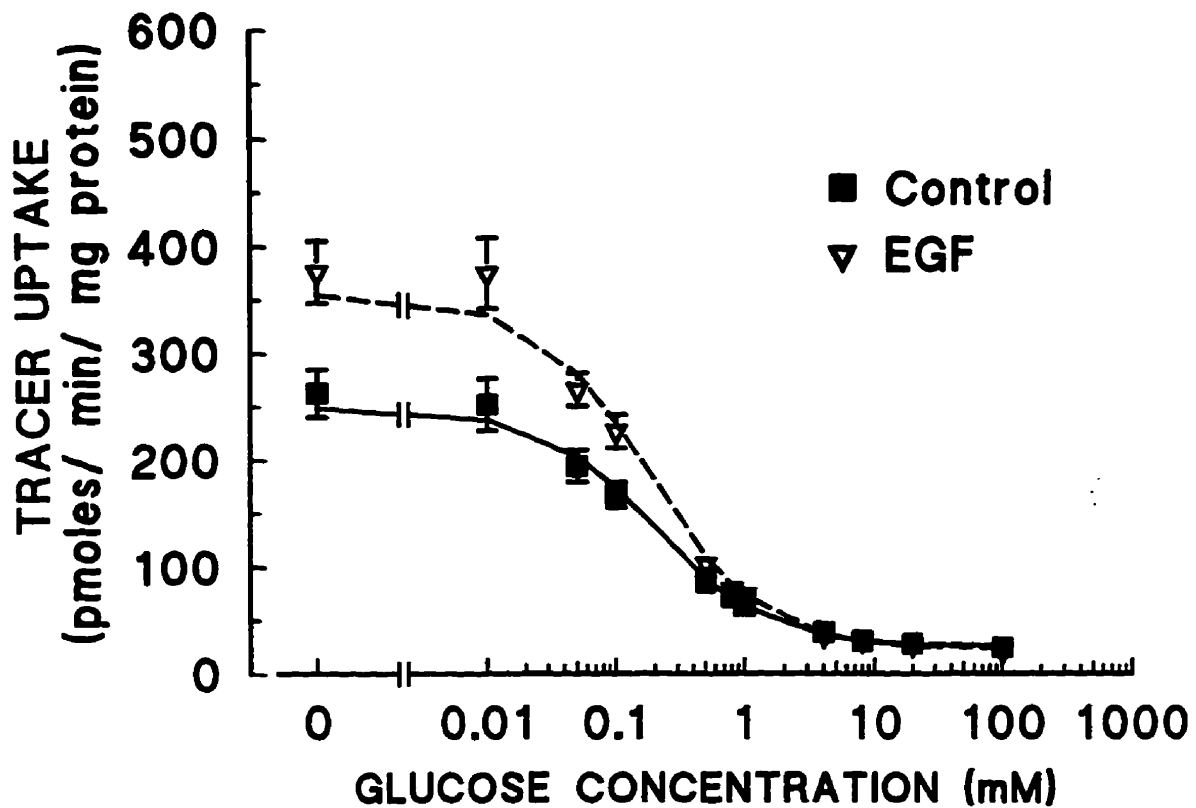


Figure VII-1. Glucose transport rates in brush border membrane vesicles obtained from EGF-treated and control tissue. Each data point represents mean  $\pm$  SE obtained in 7 membrane preparations. In each preparation measurements were performed in at least triplicate for each glucose concentration. Data shown represent the uptake of glucose in the presence of 100 mM inwardly directed sodium gradient. Rates of D- $^3$ H]glucose uptake were plotted against the concentration of unlabelled substrate present.

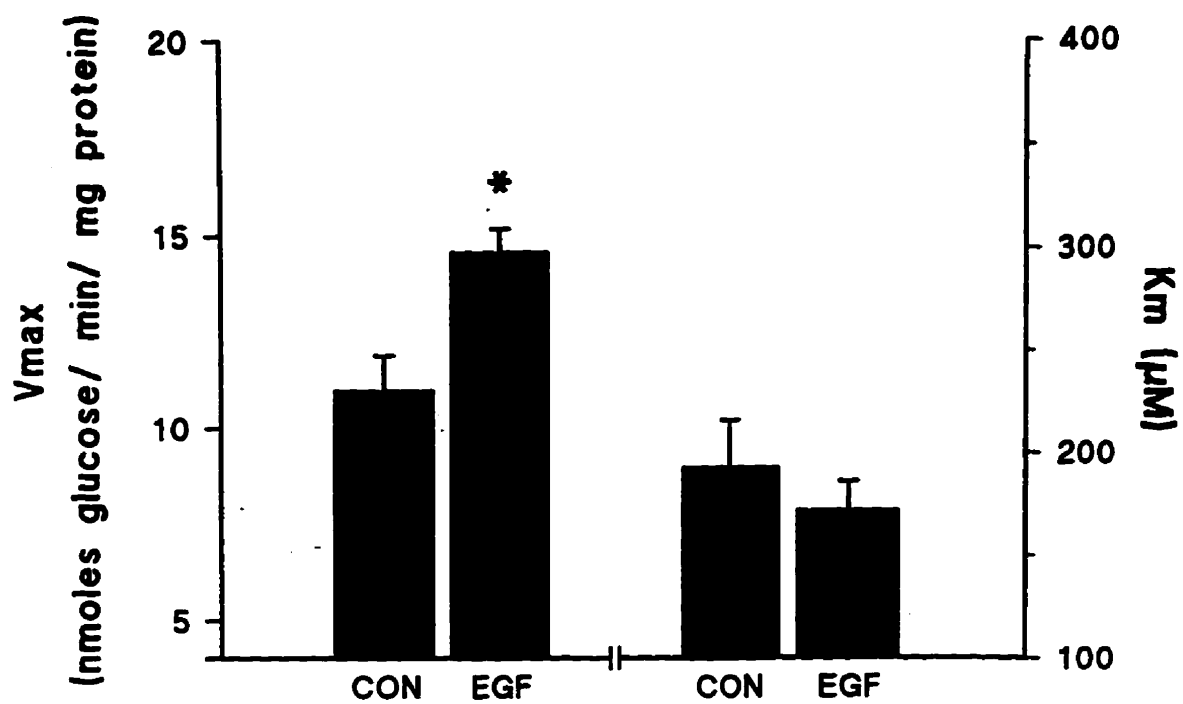


Figure VII-2. Kinetic parameters for glucose uptake into brush border membrane vesicles obtained from EGF-treated and control tissue. EGF treatment resulted in a significant increase in the Vmax for glucose uptake. Data are expressed as mean  $\pm$  S.E. n=7. \*= $p < 0.001$

D  $6.2 \pm 0.5$  vs CON  $6.3 \pm 0.5$  nmol/min/mg protein; n=4). To determine if cytochalasin D alone had any effect on brush border glucose transport kinetics, a further series of experiments was performed. As shown in Figure 4, when cytochalasin D alone was administered to loops for 1 h glucose transport kinetic values did not significantly differ compared to vesicles from control loops (Cytochalasin D  $5.5 \pm 0.5$  vs CON  $4.4 \pm 0.5$  nmol/min/mg protein; n=5). In addition, glucose  $V_{max}$  in both control and experimental vesicle preparations from both cytochalasin treatment groups was significantly ( $p < 0.001$ ) reduced compared to control values from animals not exposed to cytochalasin. No significant effect on  $K_m$  was observed compared to control in any of the three treatment groups: EGF  $172 \pm 14$   $\mu$ M vs Control  $193 \pm 23$  (Figure 2); EGF + Cytochalasin  $162 \pm 19$  vs Control  $169 \pm 16$  (Figure 3); and Cytochalasin  $138 \pm 17$  vs Control  $150 \pm 23$  (Figure 4).

## 2) Brush Border Surface Area

Representative electron micrographs of the apical brush border from the midvillus region of EGF, EGF+Cytochalasin D, and control treated loops after 1 h luminal exposure are shown in Figure 5. Brush border surface area and enterocyte ultrastructure in tissue exposed to cytochalasin alone did not differ from control therefore only control tissue is shown. No ultrastructural abnormalities were seen in any of the treatment groups. Villus and crypt architecture was unaltered and epithelial cells appeared normal showing no evidence of damage. The striking difference observed was a notable increase in microvillus height in the EGF group.





Figure VII-3. Kinetic pa  
vesicles  
tissue. Co  
increase i

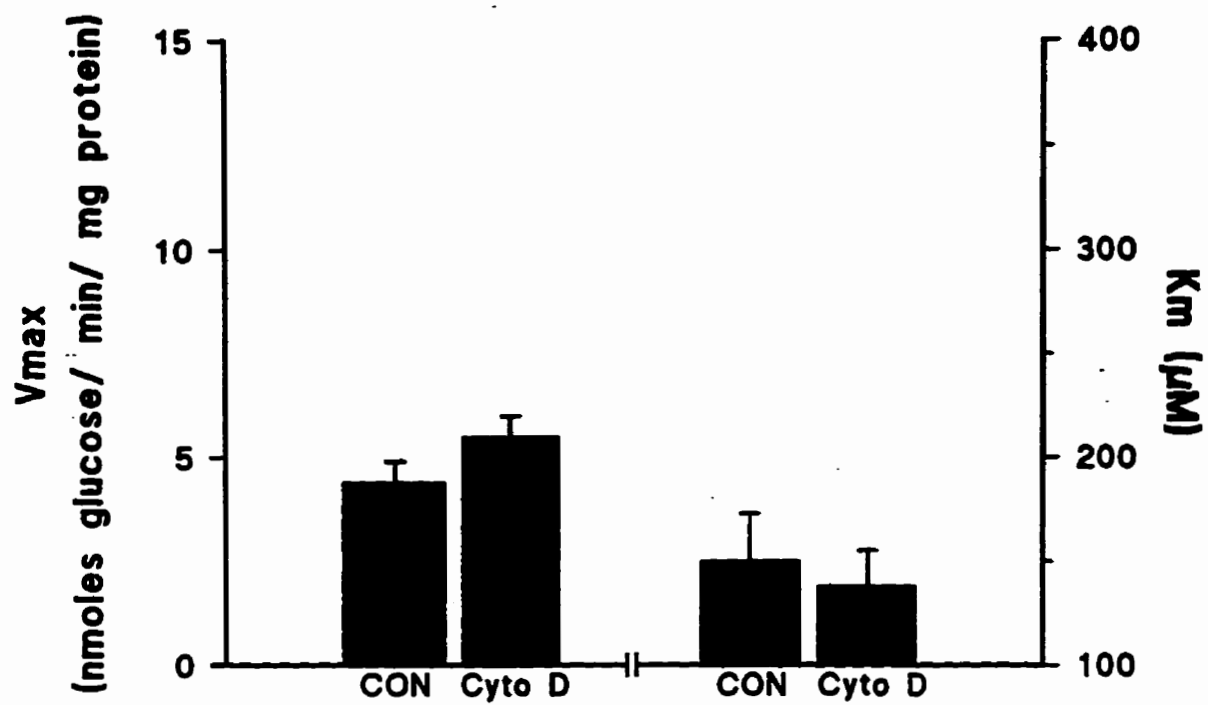


Figure VII-4. Kinetic parameters for glucose uptake into brush border membrane vesicles obtained from Cytochalasin D-treated and control tissue. Tissue treated with Cytochalasin D alone did not differ from control. Data are expressed as mean  $\pm$  S.E.  $n=5$ .

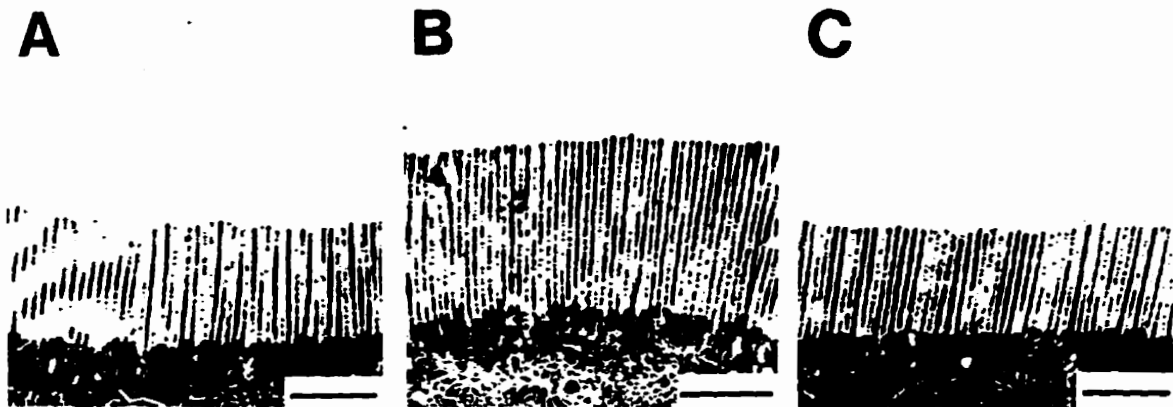


Figure VII-5. Electron micrographs of representative brush border from midvillus of A) control, B) EGF, and C) EGF + Cytochalasin D treated tissue, after loops were exposed to 1 h of the experimental solution. Tissue treated with Cytochalasin D alone did not differ from control (micrograph not shown). Bar = 1  $\mu$ m.

As shown in Figure 6 when brush border surface area was calculated, EGF (60 ng/ml) significantly ( $p < 0.001$ ) increased jejunal brush border surface area (54%) (EGF  $50.3 \pm 2.4$  vs CON  $32.6 \pm 1.3 \mu\text{m}^2$ ;  $n=26$ ). The control values for the various treatment groups examined did not significantly differ, thus, all control data were pooled. The increase in brush border surface area was due to a significant increase in microvillus height. Microvillus width and density did not significantly differ between treatment groups (Figure 6). Concurrent addition of the inhibitor of actin polymerization, cytochalasin D, abolished the increase in brush border surface area seen with EGF treatment (EGF+Cytochalasin D  $34.3 \pm 2.1$  vs CON  $32.6 \pm 1.3 \mu\text{m}^2$ ;  $n=21$ ). When the effect of cytochalasin D alone was assessed, cytochalasin D exhibited no significant effect on any brush border parameter including brush border surface area (Cytochalasin D  $39.1 \pm 3.5$  vs CON  $32.6 \pm 1.3 \mu\text{m}^2$ ;  $n=22$ ). Consistent with Madara's findings (62), treatment with cytochalasin D, either EGF+Cytochalasin D or cytochalasin D alone, appeared to result in the slight opening of tight junctions when compared to control (data not shown).

### 3) Total Surface Area

The effect of luminal EGF on total surface area was assessed using the fluorescent probe TMA-DPH. As shown in Figure 7, total absorptive surface area was significantly increased ( $p < 0.001$ ) 2.6 fold, after a 1 h exposure to EGF (EGF  $4.4 \times 10^9 \pm 0.8 \times 10^9$  vs CON  $1.7 \times 10^9 \pm 0.4 \times 10^9$ ;  $n=12$ ). To assess the role of actin in the effect of EGF on total absorptive surface area cytochalasin D (2  $\mu\text{M}$ ) was

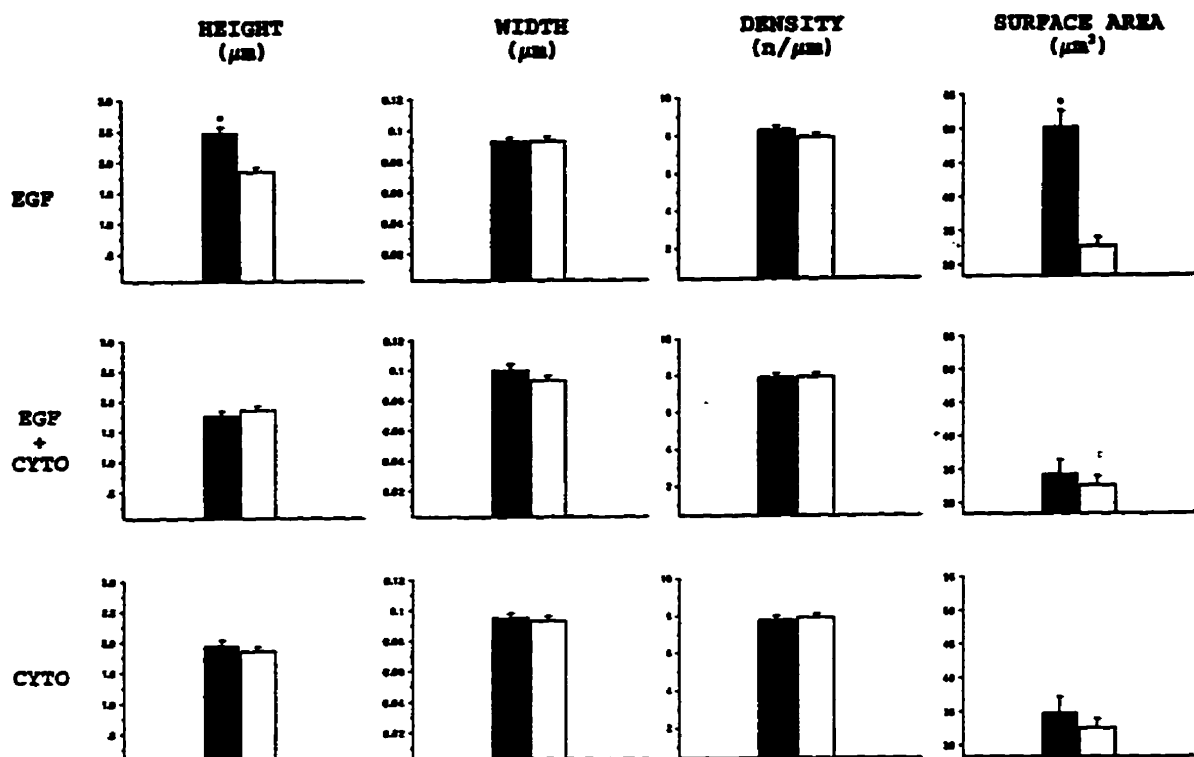


Figure VII-6. Microvillus height, width, density, and surface area of jejunal brush border from the midvillus region in EGF, EGF+Cytochalasin D, and Cytochalasin D treated tissue compared to control. Data are expressed as means  $\pm$  SE. \* $P < 0.001$ . Control data did not differ between any of the experimental groups and was therefore pooled.

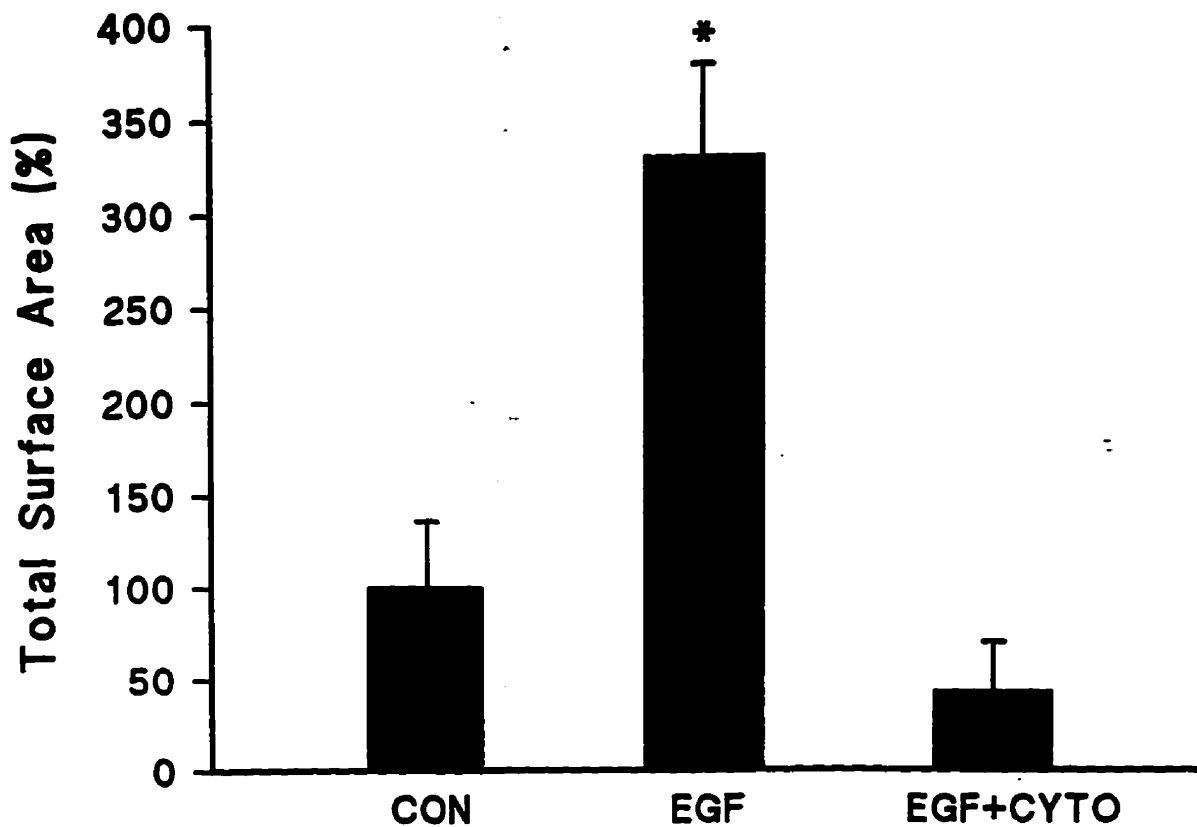


Figure VII-7. Total absorptive surface area represented as % control. In separate experiments, jejunal loops were exposed to either EGF or EGF + Cytochalasin D and compared to paired loops receiving vehicle alone. Total absorptive surface area was determined by TMA-DPH equilibration. Values are mean  $\pm$  SE of % change in surface area compared to paired control loops. \* =  $p < 0.001$

concurrently administered with EGF. The effect of EGF on total absorptive surface area was completely abolished by the concurrent administration of cytochalasin D (EGF+Cytochalasin D  $1.85 \times 10^9 \pm 0.3 \times 10^9$  vs CON  $2.5 \times 10^9 \pm 0.4 \times 10^9$ ; n=10). Total absorptive surface area in EGF+Cytochalasin D treated loops was slightly decreased (27%) from control but this effect did not achieve statistical significance ( $p > 0.1$ ).

#### **D) DISCUSSION**

The results suggest that EGF acutely upregulates jejunal brush border surface area and  $V_{max}$  for nutrient uptake through a mechanism involving actin filaments. EGF treatment resulted in a significant increase in  $V_{max}$  for brush border glucose transport, brush border surface area and total absorptive surface area. Concurrent cytochalasin D administration inhibited EGF-induced increases in glucose transport, brush border surface area, and total surface area, suggesting that actin polymerization is required for EGF-induced effects.

The cytoskeletal protein, actin, exists both as actin monomers, termed G-actin, and as long actin filaments (F-actin) composed of many polymerized monomer subunits. Following nucleation of an actin filament, subsequent elongation of the filament occurs by addition of G-actin monomers. Stability of actin filaments and their rate of growth is closely regulated and is determined by a number of factors including the free monomer concentration and a variety of actin binding proteins (2). Cytochalasin D is a fungal product which binds to and caps the ends of actin filaments inhibiting further addition of monomer subunits (2). There is some evidence that cytochalasins may also interact with G-actin monomers (95). Various roles have been characterized for actin in cellular function. Aside from its well recognized structural role as a major cytoskeletal component, actin is thought to both spatially organize cellular organelles and proteins and provide a pathway for the movement of intracellular vesicles bound to motor proteins.



As previously shown, EGF acutely upregulates brush border surface area primarily due to an increase in microvillus height and this increase in brush border surface area and microvillus height is associated with an increase in total absorptive surface area (41). Inhibition of actin polymerization by cytochalasin D abolished the EGF effects on brush border surface area and total absorptive surface area. The microvillus core is mainly composed of polymerized actin filaments, and depending on the species, 20-30 actin filaments are bundled per microvillus (9,77). There is evidence that the EGF receptor is associated with actin filaments (29,90,109), and the EGF receptor itself has been shown to bind to F-actin (29,109). Furthermore, in cell culture, EGF induces serine phosphorylation on actin causing a rapid polymerization of actin in the cytoskeleton (110) and stimulates a 30% rise in cellular filamentous actin levels (90). Of particular interest are experiments by Mooseker et al. (78) in which addition of excess G-actin induced an acute increase in microvillus length in isolated brush border preparations. Thus, alterations in actin polymerization may lead to increases in the length of the microvillus actin core, resulting in increased brush border surface area. These findings suggest that the EGF receptor and actin filaments are closely associated and suggests that EGF may exert some of its biological effects via alterations in actin pools.

There are a number of actin-binding proteins associated with the microvillus actin core (77). One protein which has been shown to be phosphorylated after EGF treatment is a 80 kDa protein termed p81 or ezrin (10,37). Ezrin is a direct EGF receptor tyrosine kinase substrate (37). EGF treatment of carcinoma A431 cells

causes phosphorylation of ezrin and the formation of microvillar-like surface structures after 30 seconds of EGF treatment, followed by membrane ruffling after 2-5 minutes (22). Ezrin is recruited into the microvillar-like structures and membrane ruffles and is tyrosine and serine phosphorylated in a time course that parallels the formation and disappearance of these surface structures. Thus, ezrin is a potential actin binding protein for mediating EGF-induced alterations in actin polymerization. Other proteins in the microvillus core that have been demonstrated to alter the equilibrium between G- and F-actin include villin, fimbrin, and fodrin (77).

Luminal EGF exposure stimulates an increase in the  $V_{\max}$  for brush border membrane glucose absorption. We have previously demonstrated that this EGF stimulated elevation in  $V_{\max}$  is not associated with any alteration in brush border membrane composition or physical characteristics (41). Furthermore, no alteration in either affinity of the  $\text{Na}^+$ -coupled cotransporter for glucose or brush border membrane sodium permeability was observed following EGF treatment (44). Thus, it seems likely that the observed elevation in glucose  $V_{\max}$  following EGF treatment is due to the cycling of additional transport proteins into the brush border membrane.

Actin has previously been implicated in the regulation of cycling and insertion of membrane proteins including transporter proteins (26,36,69,73,102,106). In T84 cells, stabilization of the actin cytoskeleton inhibited cyclic AMP stimulated  $\text{Cl}^-$  secretion suggesting a role for actin in the regulation of the cystic fibrosis conductance regulator, which is thought to mediate cAMP stimulated  $\text{Cl}^-$  secretion

(69). In MDCK cells, cytochalasin D treatment prevented endocytosis of proteins at the apical surface without affecting the basolateral surface (36). Increases in adipocyte glucose transport due to insulin are believed to occur through a translocation of glucose transporters from an intracellular pool to the cell membrane (52). Tsakiridis et al. (106) demonstrated that insulin induces a rapid reorganization of the actin cytoskeleton in rat skeletal muscle cells and that cytochalasin D treatment prevented the insulin-induced increases in glucose transport and concurrently prevented the recruitment of glucose transporters to the plasma membrane.

Our data suggests that the increase in glucose transport  $V_{max}$  and absorptive surface area induced by EGF are linked phenomena. These EGF effects appear to be due to the recruitment and insertion of a preformed pool of microvillus membrane (41). The inhibition of the EGF-induced effects produced by concurrent cytochalasin D administration may be explained by either an inhibition of actin-dependent membrane cycling and insertion or a combination of reduced vesicle trafficking and alterations in microvillus and terminal web actin polymerization.

Luminal cytochalasin D appears to exert a systemic effect. The  $V_{max}$  for glucose uptake was significantly decreased in vesicles from both experimental and control loops in EGF + cytochalasin or cytochalasin treated animals compared to control tissue from animals not exposed to cytochalasin. In contrast, brush border surface area and total absorptive surface area did not differ between any of the control groups. These data suggest cytochalasin is absorbed across the intestinal

epithelium into the circulation where it acts on downstream sites. Cytochalasin may then inhibit basal cycling of glucose transport proteins, but not membrane, into the brush border. Conversely, actin may be required for efficient functioning of the brush border sodium-glucose cotransporter. Actin has been demonstrated to play a direct role in the regulation and activity of the basolateral  $\text{Na}^+/\text{K}^+$  ATPase (4).

In summary, the findings in the current study suggest that luminal EGF acutely increases brush border surface area, total absorptive surface area and brush border glucose uptake by a mechanism dependent upon actin polymerization. Concurrent treatment with cytochalasin D, a specific inhibitor of actin polymerization, abolishes EGF-induced increases in both apical surface area and glucose transport indicating that the observed increases in microvillus height and recruitment of absorptive membrane and transport proteins are linked phenomena.

## VIII. SUMMARY

Production and secretion of EGF in the gastrointestinal tract mainly occurs from the salivary and Brunner's glands (68). In the presence of food, EGF is resistant to degradation, reaching luminal concentrations as high as 100 ng/ml (86). The presence of EGF receptors has been reported throughout the small intestine (104), and EGF has been shown to upregulate nutrient absorption (49,82) suggesting that EGF plays a role in the regulation of nutrient absorption in the gastrointestinal tract.

These studies demonstrate activation of the epidermal growth factor receptor via EGF results in increased brush border nutrient absorption. The mechanisms involved in EGF-induced increases in nutrient transport were dependent on both tyrosine kinase activity and actin polymerization. Epidermal growth factor induced increases in brush border surface area and total absorptive surface area were also dependent on actin polymerization.

The ability of an actin depolymerizing agent to inhibit both EGF induced increases in glucose  $V_{max}$  and absorptive surface area suggests that the two processes are linked. Furthermore, the EGF effect requires tyrosine kinase activity suggesting a role for the EGF receptor in mediating the actions of EGF.

In summary, EGF upregulates nutrient absorption by a mechanism that involves tyrosine kinase. Furthermore, upregulation of BBSA and nutrient absorption by EGF is also dependent on actin polymerization. Insights into the mechanisms

**regulating brush border surface area may allow for therapeutic modulation of absorptive surface area, thereby providing an effective treatment for nutritional and diarrheal disorders.**

## **IX. FUTURE DIRECTIONS OF RESEARCH**

The findings in these studies suggest that EGF increases brush border surface area and nutrient absorption by mechanisms that involve tyrosine kinase activity and actin polymerization. From these studies, a number of additional experiments could be performed, to further define the mechanisms involved in EGF increases in induced nutrient absorption.

The EGF receptor possesses intrinsic tyrosine kinase activity. In this study, tyrphostin 51, a non-specific inhibitor of tyrosine kinase activity, was used. Studies using truncated forms of the EGF receptor with absent or non-functional tyrosine kinase activity indicate EGF requires an intact functional EGF receptor tyrosine kinase to exert its effects. A more specific inhibitor of the EGF receptor tyrosine kinase could be used to define the specific tyrosine kinase or kinases involved in EGF signal transduction.

EGF has been shown to activate a variety of different target proteins depending on the cell type. One enzyme reported to be activated by EGF is phospholipase C<sub>γ</sub> (PLC<sub>γ</sub>), which cleaves phosphatidylinositol bisphosphate (PIP<sub>2</sub>) producing the second messengers, inositol triphosphate (IP<sub>3</sub>), and diacylglycerol (DAG) (84). IP<sub>3</sub> then liberates Ca<sup>2+</sup> from intracellular stores and DAG activates protein kinase C (PKC), which is a serine/threonine kinase. The EGF induced alterations in nutrient transport have been shown to be dependent on the presence of extracellular Ca<sup>2+</sup>, as administration of the Ca<sup>2+</sup> channel blocker, verapamil,

abolishes the EGF effect (82). Furthermore, administration of EGF has been shown to cause phosphorylation of serine and threonine residues on actin filaments (110). It would be useful to identify the EGF signal transduction mechanism in the enterocyte. Specifically, the use of an inhibitor of PLC $\gamma$  concurrent with EGF treatment on enterocytes would further the understanding of EGF signal transduction in the enterocyte.

In order to acutely increase absorptive surface area a preformed membrane pool with functional transporters must be present within the cell. Upon stimulation with EGF, this preformed pool of membrane must quickly insert into the brush border membrane as the length of the microvillus core increases. Thus, studies could be initiated to examine the location of the preformed membrane pool and the transporters within the pool. Studies could be performed using anti SGLT1 antibody to identify the location of the preformed membrane pool and the glucose transporter.

Many intracellular transport processes use both the microtubular network and actin filaments (2). The insertion of the preformed pool of membrane and transporters may be mediated by microtubules, actin filaments, or a combination of both. Colchicine, an inhibitor of microtubule polymerization, could be used to probe the role of microtubules in the EGF effect.

Clearly, the ideas proposed above are not exhaustive. Additionally, the results obtained in one series of experiments may shed light on further avenues of investigation in this exciting area of gastrointestinal physiology.



## **X. REFERENCES**

1. Adams, R. J. and T. D. Pollard. 1986. Propulsion of organelles isolated from *Acanthamoeba* along actin filaments by myosin-I. *Nature* 322:754-756.
2. Alberts, B., D. Bray, J. Lewis, M. Raff, K. Roberts, and J. D. Watson. 1994. The cytoskeleton. In *Molecular biology of the cell*. Garland Publishing Inc., New York & London. 797-861.
3. Barnard, J. A., R. D. Beauchamp, W. E. Russell, R. N. Dubois, and R. J. Coffey. 1995. Epidermal Growth Factor-Related Peptides and Their Relevance to Gastrointestinal Pathophysiology. *Gastroenterology* 108:564-580.
4. Bertorello, A. M. and A. I. Katz. 1995. Regulation of Na<sup>+</sup>-K<sup>+</sup> pump activity: pathways between receptors and effectors. *NIPS* 10:253-259.
5. Bird, A. R., W. J. Croom, Y. K. Fan, L. R. Daniel, B. L. Black, B. W. McBride, E. J. Eisen, L. S. Bull, and I. L. Taylor. 1994. Jejunal glucose absorption is enhanced by epidermal growth factor in mice. *J. Nutr.* 124:231-240.
6. Bischof, G., B. Illek, W. W. Reenstra, and T. E. Machen. 1995. Role of tyrosine kinases in carbachol-regulated Ca entry into colonic epithelial cells. *Am. J. Physiol.* 268:C154-C161.

7. Boonstra, J., P. J. Rijken, B. Humbel, F. Cremers, A. J. Verkleij, and P. M. P. Van Bergen en Henegouwen. 1995. The epidermal growth factor. *Cell Biology International* 19:413-430.
8. Bradbury, N. A. and R. J. Bridges. 1994. Role of membrane trafficking in plasma membrane solute transport. *Am. J. Physiol.* 267:C1-C24.
9. Bretscher, A. 1991. Microfilament structure and function in the cortical cytoskeleton. *Ann. Rev. Cell Biol.* 7:337-374.
10. Bretscher, A. 1993. Microfilaments and membranes. *Current Opinion in Cell Biology* 5:653-660.
11. Broschat, K. O., R. P. Stidwill, and D. R. Burgess. 1983. Phosphorylation controls brush border motility by regulating myosin structure and association with the cytoskeleton. *Cell* 35:561-571.
12. Brown, S. S. and J. A. Spudich. 1979. Cytochalasin inhibits the rate of elongation of actin filament fragments. *J. Cell Biol.* 83:657-662.
13. Buret, A., D. G. Gall, and M. E. Olson. 1991. Growth, activities of enzymes in

the small intestine, and ultrastructure of the microvillous border in gerbils infected with *Giardia duodenalis*. *Parasitol. Res.* 77:109-114.

14. Buret, A., E. V. O'Loughlin, G. Curtis, and D. G. Gall. 1990. Effect of acute *Yersinia enterocolitica* infection on small intestinal ultrastructure. *Gastroenterology* 98:1401-1407.

15. Buschmann, R. J. 1983. Morphometry of the small intestinal enterocytes of the fasted rat and the effects of colchicine. *Cell Tissue Res.* 231:289-299.

16. Campos-Gonzalez, R. and J. R. Glenney. 1992. Tyrosine phosphorylation of mitogen-activated protein kinase in cells with tyrosine kinase-negative epidermal growth factor receptors. *J. Biol. Chem.* 267:14535-14538.

17. Canals, F. 1992. Signal transmission by epidermal growth factor receptor: coincidence of activation and dimerization. *Biochemistry* 31:4493-4501.

18. Carpenter, G. and S. Cohen. 1979. Epidermal growth factor. *Ann. Rev. Biochem.* 48:193-216.

19. Carpenter, G. and S. Cohen. 1990. Epidermal Growth Factor. *J. Biol. Chem.* 265:7709-7712.

20. Chang, E. B., M. D. Sitrin, and D. D. Black. 1996. *Gastrointestinal, Hepatobiliary, and Nutritional Physiology*. Lippincott-Raven Publishers, Philadelphia.

21. Cheeseman, C. I. and D. D. Maenz. 1989. Rapid regulation of D-glucose transport in basolateral membrane of rat jejunum. *Am. J. Physiol.* 256:G878-G883.

22. Chinkers, M., J. M. McKanna, and S. Cohen. 1979. Rapid induction of morphological changes in human carcinoma cells A-431 by epidermal growth factor. *J. Cell Biol.* 83:260-265.

23. Cooper, J. A. 1987. Effects of cytochalasin and phalloidin on actin. *J. Cell Biol.* 105:1473-1478.

24. Cooperstein, C. J. and A. Lazarow. 1951. A microspectrophotometric method for the determination of cytochrome oxidase. *J. Biol. Chem.* 189:665-670.

25. Curtis, G. H., M. K. Patrick, A. G. Catto-Smith, and D. G. Gall. 1990. Intestinal anaphylaxis in the rat. *Gastroenterology* 98:1558-1566.

26. Cushman, S. W. and L. J. Wardzala. 1980. Potential mechanism of insulin

action on glucose transport in the isolated rat adipose cell. *J. Biol. Chem.* 255:4758-4762.

27. Dalquist, A. 1964. Method for assay of intestinal disaccharidases. *Anal. Biochem.* 7:18-25.

28. Defize, L. H. K., J. Boonstra, J. Meisenhelder, W. Kruijer, L. G. J. Tertoolen, B. C. Tilly, T. Hunter, P. M. P. Van Bergen en Henegouwen, W. Moolenaar, and S. W. de Laat. 1989. Signal transduction by epidermal growth factor occurs through the subclass of high affinity receptors. *J. Biol. Chem.* 109:2495-2507.

29. den Hartigh, J. C., P. M. P. Van Bergen en Henegouwen, A. J. Verkleij, and J. Boonstra. 1992. The EGF receptor is an actin-binding protein. *J. Cell Biol.* 119:349-355.

30. Donowitz, M., J. L. M. Montgomery, M. S. Walker, and M. E. Cohen. 1994. Brush-border tyrosine phosphorylation stimulates ileal neutral NaCl absorption and brush-border  $\text{Na}^+/\text{H}^+$  exchange. *Am. J. Physiol.* 266:G647-G656.

31. Dvir, A., Y. Milner, O. Chomsky, C. Gilon, A. Gazit, and A. Levitzki. 1991. The inhibition of EGF-dependent proliferation of keratinocytes by tyrosine kinase blockers. *J. Cell Biol.* 113:857-865.

32. Forte, J. G., D. K. Hanzel, C. Okamoto, D. Chow, and T. Urushidani. 1990. Membrane and protein recycling associated with gastric HCL secretion. *Journal of Internal Medicine* 228:17-26.
33. Friederich, E., E. Pringault, M. Arpin, and D. Louvard. 1990. From the structure to the function of villin, an actin-binding protein of the brush border. *Bioessays* 12:403-408.
34. Ganapathy, V., M. Brandsch, and F. H. Leibach. 1994. Intestinal transport of amino acids and peptides. In *Physiology of the Gastrointestinal Tract, Third Edition*. L. R. Johnson, editor. Raven Press, New York. 1773-1794.
35. Gazit, A., P. Yaish, C. Gilon, and A. Levitzki. 1989. Tyrphostins I: synthesis and biological activity of protein tyrosine kinase inhibitors. *J. Med. Chem.* 32:2344-2352.
36. Gottlieb, T. A., I. E. Ivanov, M. Adesnik, and D. D. Sabatini. 1993. Actin microfilaments play a critical role in endocytosis at the apical but not the basolateral surface of polarized epithelial cells. *J. Cell Biol.* 120:695-710.
37. Gould, K. L., J. A. Cooper, A. Bretscher, and T. Hunter. 1986. The protein-tyrosine kinase substrate, p81, is homologous to a chicken microvillar core

protein. *J. Cell Biol.* 102:660-669.

38. Gregory, H. 1985. In vivo aspects of urogastrone-epidermal growth factor. *J. Cell Sci.* 3:11-17.

39. Hanzel, D. K., H. Reggio, A. Bretscher, J. G. Forte, and P. Mangeat. 1991. The secretion-stimulated 80K phosphoprotein of parietal cells is ezrin, and has properties of a membrane cytoskeletal linker in the induced apical microvilli. *EMBO* 10:2363-2373.

40. Hanzel, D. K., T. Urushidani, W. R. Usinger, A. Smolka, and J. G. Forte. 1989. Immunological localization of an 80-kDa phosphoprotein to the apical membrane of gastric parietal cells. *Am. J. Physiol.* 256:G1082-G1089.

41. Hardin, J. A., A. Buret, J. B. Meddings, and D. G. Gall. 1993. Effect of epidermal growth factor on enterocyte brush-border surface area. *Am. J. Physiol.* 264:G312-G318.

42. Hardin, J. A. and D. G. Gall. 1992. The Regulation of Brush Border Surface Area. *Annals of the New York Academy of Sciences* 664:380-387.

43. Hardin, J. A. and D. G. Gall. 1992. The effect of TGF on intestinal solute

transport. *Regulatory Peptides* 39:169-176.

44. Hardin, J. A., J. K. Wong, C. I. Cheeseman, and D. G. Gall. 1996. The effect of luminal epidermal growth factor on enterocyte glucose and proline transport. *Am. J. Physiol.* 271:G509-G515.

45. Hinterleitner, T. A. and D. W. Powell. 1991. Immune system control of intestinal ion transport. *Proc. Soc. Exp. Biol. Med.* 197:249-260.

46. Hollenberg, M. D. 1994. Tyrosine kinase pathways and the regulation of smooth muscle contractility. *TiPS* 15:108-114.

47. Hollenberg, M. D. 1995. Tyrosine kinase-mediated signal transduction pathways and the actions of polypeptide growth factors and G-protein-coupled agonists in smooth muscle. *Molecular and Cellular Biochemistry* 149/150:77-85.

48. Holmes, R. and R. W. Loble. 1989. Intestinal brush border revisited. *Gut* 30:1667-1678.

49. Horvath, K., I. D. Hill, P. Devarajan, D. Mehta, S. C. Thomas, R. B. Lu, and E. Lebenthal. 1994. Short-term effect of epidermal growth factor (EGF) on sodium and glucose cotransport of isolated jejunal epithelial cells. *Biochim. Biophys. Acta*



1222:215-222.

50. Hubel, K. A. 1989. Control of intestinal secretion. In *Gastrointestinal Secretion*. J. S. Davison, editor. Butterworth & Co. Ltd., London. 178-201.

51. Ino, M., K. Ushiro, C. Ino, T. Yamashita, and T. Kumazawa. 1993. Kinetics of epidermal growth factor in saliva. *Acta Otolarygol. (Stockh. ) Suppl.* 500:126-130.

52. Joost, H. G., T. M. Weber, and S. W. Cushman. 1988. Qualitative and quantitative comparison of glucose activity and glucose transporter concentration in plasma membranes from basal and insulin-stimulated rat adipose cells. *Biochem. J.* 249:155-161.

53. Jourd'Heuil, D., P. Vaananen, and J. B. Meddings. 1993. Lipid peroxidation of the brush border membrane: membrane physical properties and glucose transport. *Am. J. Physiol.* 264:G1009-G1015.

54. Kelly, M., D. G. Butler, and J. R. Hamilton. 1972. Transmissible gastroenteritis in piglets: a model of infantile viral diarrhea. *J. Pediatr.* 80:925-931.

55. Kessler, M., O. Acuto, C. Storelli, H. Murer, M. Muller, and G. Semenza. 1978. A modified procedure for the rapid preparation of efficiently transporting vesicles

from small intestinal brush border membranes. Their use in investigating some properties of D-glucose and choline transport systems. *Biochim. Biophys. Acta* 771:35-41.

56. Koepsell, H. and J. Spangenberg. 1994. Function and Presumed Molecular Structure of Na<sup>+</sup>-D-Glucose Cotransport Systems. *J. Membrane Biol.* 138:1-11.

57. Lange, Y., M. H. Swaisgood, B. V. Ramos, and T. L. Steck. 1989. Plasma membranes contain half the phospholipid and 90% of the cholesterol and sphingomyelin in cultured human fibroblasts. *J. Biol. Chem.* 264(7):3786-3793.

58. Lecount, T. S. and R. D. Gray. 1972. Transient shortening of microvilli induced by cycloheximide in the duodenal epithelium of the chicken. *J. Cell Biol.* 53:601-605.

59. Lipkin, M. 1987. Proliferation and Differentiation of Normal and Diseased Gastrointestinal Cells. In *Physiology of the Gastrointestinal Tract*. L. R. Johnson, editor. Raven Press, New York. 255-284.

60. Louvard, D., M. Kedinger, and H. P. Hauri. 1992. The differentiating epithelial cell: establishment and maintenance of functions through interactions between cellular structures. *Ann. Rev. Cell Biol.* 8:157-195.

61. Lowry, O. H., N. J. Rosebrough, A. L. Farr, and R. J. Randall. 1951. Protein measurement with the Folin phenol reagent. *J. Biol. Chem.* 193:265-257.
62. Madara, J. L., D. Barenberg, and S. Carlson. 1986. Effects of cytochalasin D on occluding junctions of the intestinal absorptive cells: Further evidence that the cytoskeleton may influence paracellular permeability and junctional charge selectivity. *J. Cell Biol.* 102:2125-2136.
63. Madara, J. L. and J. S. Trier. 1994. The functional morphology of the mucosa of the small intestine. In *Physiology of the Gastrointestinal Tract, Third Edition*. L. R. Johnson, editor. Raven Press, New York. 1577-1622.
64. Maenz, D. D. and C. I. Cheeseman. 1986. Effect of hyperglycemia on D-glucose transport across the brush-border and basolateral membrane of the small intestine. *Biochim. Biophys. Acta* 860:277-285.
65. Maenz, D. D. and C. I. Cheeseman. 1987. The Na<sup>+</sup>-independent D-glucose transporter in the enterocyte basolateral membrane: orientation and cytochalasin B binding characteristics. *J. Membrane Biol.* 97:259-266.
66. Malo, C. and A. Berteloot. 1991. Analysis of kinetic data in transport studies: New insights from kinetic studies of Na<sup>+</sup>-D-Glucose cotransport in human intestinal

brush-border membrane vesicles using a fast sampling, rapid filtration apparatus. *J. Membrane Biol.* 122:127-141.

67. Maroux, S., E. Coudrier, H. Feracci, J. P. Gorvel, and D. Louvard. 1988. Molecular organization of the intestinal brush border. *Biochimie* 70:1297-1306.

68. Marti, U., S. J. Burwen, and A. L. Jones. 1989. Biological effects of epidermal growth factor, with emphasis on the gastrointestinal tract and liver: an update. *Hepatology* 9:126-138.

69. Mathews, J. B., C. S. Awtrey, and J. L. Madara. 1992. Microfilament-dependent activation of Na/K/2Cl cotransport by cAMP in intestinal epithelial monolayers. *J. Clin. Invest* 90:1608-1613.

70. Meddings, J. B., D. DeSouza, M. Goel, and S. Thiesen. 1990. Glucose transport and the microvillus membrane Physical properties along the crypt-villus axis of the rabbit. *J. Clin. Invest* 85:1099-1107.

71. Meddings, J. B., R. B. Scott, and G. H. Fick. 1989. Analysis and comparison of sigmoidal curves: application to dose-response data. *Am. J. Physiol.* 257:G982-G989.

72. Mills, J. W. and L. J. Mandel. 1994. Cytoskeletal regulation of membrane transport events. *FASEB J.* 8:1161-1165.
73. Mills, J. W., E. M. Schwiebert, and B. A. Stanton. 1994. The cytoskeleton and membrane transport. *Current Opinion in Nephrology and Hypertension* 3:529-534.
74. Misch, D., P. E. Giebel, and R. G. Faust. 1980. Intestinal microvilli: responses to feeding and fasting. *European Journal of Cell Biology* 21:269-279.
75. Moolenaar, W., A. J. Bierman, B. C. Tilly, I. Verlaan, L. H. K. Defize, A. M. Honegger, A. Ullrich, and J. Schlessinger. 1988. A point mutation at the ATP-binding site of the EGF receptor abolishes signal transduction. *EMBO* 7:707-710.
76. Mooseker, M. S. 1976. Brush border motility. Microvillar contraction in triton-treated brush borders isolated from the intestinal epithelium. *J. Cell Biol.* 71:417-433.
77. Mooseker, M. S. 1985. Organization, chemistry, and assembly of the cytoskeletal apparatus of the intestinal brush border. *Ann. Rev. Cell Biol.* 1:209-241.
78. Mooseker, M. S., T. D. Pollard, and K. A. Wharton. 1982. Nucleated

**polymerization of actin from the membrane associated ends of microvillar filaments in the intestinal brush border. J. Cell Biol. 95:223-233.**

**79. O'Loughlin, E. V. and D. G. Gall. 1989. Small intestinal absorption and secretion of fluid and electrolytes. In Gastrointestinal Secretion. J. S. Davison, editor. Butterworth and Co. Ltd., London. 157-170.**

**80. O'Loughlin, E. V., C. H. Pai, and D. G. Gall. 1988. Effect of acute Yersinia enterocolitica infection on In vivo and In vitro small intestinal solute and fluid absorption in the rabbit. Gastroenterology 94:664-672.**

**81. Ohmori, H. and S. Toyama. 1992. Direct proof that the primary site of action of cytochalasin on cell motility processes is actin. J. Cell Biol. 116:933-941.**

**82. Opleta-Madsen, K., J. A. Hardin, and D. G. Gall. 1991. Epidermal growth factor upregulates intestinal electrolyte and nutrient transport. Am. J. Physiol. 260:G807-G814.**

**83. Parkinson, D. K., H. Ebel, D. R. Dibona, and G. W. Sharp. 1972. Localization of the action of the cholera toxin on adenyl cyclase in mucosal epithelial cells of rabbit intestine. J. Clin. Invest 51:2292-2298.**

84. Payraastre, B., P. M. P. Van Bergen en Henegouwen, M. Breton, J. C. den Hartigh, M. Plantavid, A. J. Verkleij, and J. Boonstra. 1991. Phosphoinositide kinase, diacylglycerol kinase, and phospholipase C activities associated to the cytoskeleton: effect of epidermal growth factor. *J. Cell Biol.* 115:121-128.
85. Playford, R. J., T. Marchbank, D. P. Calnan, J. Calam, P. Royston, J. J. Batten, and H. F. Hansen. 1995. Epidermal Growth Factor is digested to smaller, less active forms in acidic gastric juice. *Gastroenterology* 108:92-101.
86. Playford, R. J., A. C. Woodman, P. Clark, P. Watanapa, D. Vesey, P. H. Deprez, R. C. N. Williamson, and J. Calam. 1993. Effect of luminal growth factor preservation on intestinal growth. *Lancet* 341:843-848.
87. Pollard, T. D. and S. W. Craig. 1982. Mechanism of actin polymerization. *TIBS* 55-58.
88. Pouslen, S. S., E. Nexø, P. Skov Olsen, J. Hess, and P. Kirkegaard. 1986. Immunohistochemical localization of epidermal growth factor in rat and man. *Histochemistry* 85:389-394.
89. Rijken, P. J., W. J. Hage, P. M. P. Van Bergen en Henegouwen, A. J. Verkleij, and J. Boonstra. 1991. Epidermal growth factor induces rapid reorganization of the

**actin microfilament system in human A431 cells. J. Cell Sci. 100:491-499.**

**90. Rijken, P. J., S. M. Post, W. J. Hage, P. M. P. Van Bergen en Henegouwen, A. J. Verkleij, and J. Boonstra. 1995. Actin polymerization localizes to the activated epidermal growth factor receptor in the plasma membrane, independent of the cytosolic free calcium transit. Exp. Cell Res. 218:223-232.**

**91. Rodewald, R., S. B. Newman, and M. J. Karnovsky. 1976. Contraction of isolated brush borders from the intestinal epithelium. J. Cell Biol. 70:541-554.**

**92. Rood, R. P., E. Emmer, J. Wesolek, J. McCullen, Z. Husain, M. E. Cohen, R. S. Braithwaite, H. Murer, G. W. G. Sharp, and M. Donowitz. 1988. Regulation of the rabbit ileal brush-border Na<sup>+</sup>/H<sup>+</sup> exchanger by an ATP-requiring Ca<sup>2+</sup>/calmodulin-mediated process. J. Clin. Invest 82:1091-1097.**

**93. Sadowski, D. C., D. J. Gibbs, and J. B. Meddings. 1992. Proline transport across the intestinal microvillus membrane may be regulated by membrane physical properties. Biochim. Biophys. Acta 1105:75-83.**

**94. Salloum, R. M., B. R. Stevens, G. S. Schultz, and W. W. Souba. 1993. Regulation of small intestinal glutamine transport by epidermal growth factor. Surgery 113:552-559.**



95. Sampath, P. and T. D. Pollard. 1991. Effects of cytochalasin, phalloidin, and pH on the elongation of actin filaments. *Biochemistry* 30:1973-1980.

96. Schwartz, M. Z. and R. B. Storozuk. 1988. Influence of epidermal growth factor on intestinal function in the rat: comparison of systemic infusion versus luminal perfusion. *American Journal of Surgery* 155:18-22.

97. Sodring Elbrond, V., V. Dantzer, T. M. Mayhew, and E. Skadhauge. 1991. Avian lower intestine adapts to dietary salt (NaCl) depletion by increasing transepithelial sodium transport and microvillus membrane surface area. *Exper. Physiol.* 76:733-744.

98. Sottocasa, G. L., B. Kuylensturna, L. Ernster, and A. Bergstrand. 1967. An electron transport system associated with the outer membrane of liver mitochondria. A biochemical and morphological study. *J. Cell Biol.* 32:1112-1124.

99. Spaargaren, M., L. H. K. Defize, J. Boonstra, and S. W. de Laat. 1991. Antibody-induced dimerization activates the epidermal growth factor receptor tyrosine kinase. *J. Biol. Chem.* 266:1733-1739.

100. Stagsted, J., S. Ziebe, S. Satoh, G. D. Holman, S. W. Cushman, and L. à

Olsson. 1993. Insulinomimetic effect on glucose transport by epidermal growth factor when combined with a major histocompatibility complex class I-derived peptide. *J. Biol. Chem.* 268:1770-1774.

101. Stidwell, R. P. and D. R. Burgess. 1986. Regulation of intestinal brush border microvillus length during development by the G- to F-actin ratio. *Developmental Biology* 114:381-388.

102. Suzuki, K. and T. Kono. 1980. Evidence that insulin causes translocation of glucose transport activity to the plasma membrane from an intracellular storage site. *Proc. Natl. Acad. Sci.* 77:2542-2445.

103. Takata, K., T. Kasahara, M. Kasahara, O. Ezaki, and H. Hirano. 1992. Immunohistochemical localization of Na<sup>+</sup>-dependent glucose transporter in the jejunum. *Cell Tissue Res* 267:3-9.

104. Thompson, J. F. 1988. Specific receptors for epidermal growth factor in rat intestinal microvillus membranes. *Am. J. Physiol.* 254:G429-G435.

105. Thompson, J. F., R. M. Lamprey, and P. C. Stokkers. 1993. Orogastric EGF enhances c-neu and EGF receptor phosphorylation in suckling rat jejunum in vivo. *Am. J. Physiol.* 265:G63-G72.

106. Tsakiridis, T., M. Vranic, and A. Klip. 1994. Disassembly of the Actin Network Inhibits Insulin-dependent Stimulation of Glucose Transport and Prevents Recruitment of Glucose Transporters to the Plasma Membrane. *J. Biol. Chem.* 269:29934-29942.

107. Tsang, R., Z. Ao, and C. I. Cheeseman. 1994. Influence of vascular and luminal hexoses on rat intestinal basolateral glucose transport. *Can. J. Physiol. Pharmacol.* 72:317-326.

108. Ullrich, A. and J. Schlessinger. 1990. Signal transduction by receptors with tyrosine kinase activity. *Cell* 61:203-212.

109. Van Bergen en Henegouwen, P. M. P., J. C. den Hartigh, P. Romeyn, A. J. Verkleij, and J. Boonstra. 1992. The epidermal growth factor receptor is associated with actin filaments. *Exp. Cell Res.* 199:90-97.

110. van Delft, S., A. J. Verkleij, J. Boonstra, and P. M. P. Van Bergen en Henegouwen. 1995. Epidermal growth factor induces serine phosphorylation of actin. *FEBS Lett.* 357:251-254.

111. Venable, J. H. and R. Coggeshall. 1965. A simplified lead citrate stain for use

in electron microscopy. *J. Cell Biol.* 25:407-408.

112. Watson, A. J. M., S. Levine, M. Donowitz, and M. H. Montrose. 1992. Serum regulates Na<sup>+</sup>/H<sup>+</sup> exchange in Caco-2 cells by a mechanism which is dependent on F-actin. *J. Biol. Chem.* 267:956-962.

113. Wild, G. E. and A. B. R. Thomson. 1996. Alterations in Na/Glucose Cotransporter (SGLT1) Gene Expression in Crohn's Ileitis. *Gastroenterology* 110:A1044.(Abstr.)

114. Wright, E. M., B. Hirayama, D. D. Loo, E. Turk, and K. Hager. 1994. Intestinal sugar transport. In *Physiology of the Gastrointestinal Tract, Third Edition*. L. R. Johnson, editor. Raven Press, New York. 1751-1772.